Structural Design of the X-15

R. L. SCHLEICHER, D.Sc., A.F.A.I.A.A.

Manager Structures Engineering, Los Angeles Division, North American Aviation, Inc.

The 1346th Lecture to be delivered before the Society, "Structural Design of the X-15", by Dr. R. L. Schleicher, was given on 18th April 1963 in the Society's Lecture Theatre with Mr. B. S. Shenstone, M.A.Sc., F.R.Ae.S., F.A.I.A.A., F.C.A.S.I., in the Chair. Introducing the lecturer, Mr. Shenstone said that Dr. Schleicher was Manager, Structures Engineering, at the Los Angeles Division of North American Aviation, Inc., and he had been with the firm since its inception in 1934. Dr. Schleicher was a graduate of Villanova University and held a degree of B.S. in M.E., and his D.Sc. had been conferred on him in 1957. He had nearly 34 years experience in aircraft structures engineering beginning in 1929. He had been Chief Structures Engineer at North American Aviation, Inc. on all the aircraft designed and built by the Los Angeles Division of that company and that included the X-15. He was a member of the Society for Experimental Stress Analysis and an Associate Fellow of the A.I.A.A. From 1943 to 1958 he had been a member of a number of NACA (now NASA) Committees and Sub-committees and had written a number of technical papers. He was currently serving on an Advisory Committee on Aircraft Structures for the U.S. Air Forces.

They were indeed grateful to Dr. Schleicher for coming all this way to lecture.

Introduction

While most extra-terrestrial interest today is centred on achievements in space, a hypersonic flight research programme, involving a group of manned aircraft, is being conducted over the California desert in the U.S.A. This programme has proved to be most fruitful after nearly four years of operation. Begun in 1955, the design and construction of this aircraft represented a distinct advancement in the state of the art and has proved the value of aeronautical research involving piloted aircraft. Since practically all of the basic research in both materials and structural science to make this aircraft possible had been completed, there remained the engineering and manufacturing problems to be solved. In less than three years and after the expenditure of many engineering man hours, there emerged the first of three research air vehicles built for the purpose of conducting hypersonic flight tests. The three aircraft were built at the Los Angeles Division of North American Aviation, Inc. for the United States Air Force to be operated by the National Aeronautics and Space Administration at its High Speed Flight Station at Edwards Air Force Base in California. As indicated by the title, the structural design including materials of construction of the X-15, will be discussed in this paper. Some of the more interesting problems that arose in connection with the design and construction are presented.

Air Vehicle Description

The X-15 is a single-place, mid-wing monoplane designed to explore the areas of stability, control, high aerodynamic heating rates, physiological phenomena, and other problems related to hypersonic flight. In appearance it is characterised by a long cylindrical fuselage with pointed nose and side fairings, a short tapered wing located well aft, a horizontal tail having marked cathedral, a wedge shaped vertical tail with dive brakes extending above and below the fuselage, a landing gear composed of two retractable skids located at the extreme aft end of the fuselage, and a nose gear located in the nose (Fig. 2). Two control systems are used; one for operation within the atmosphere and one for use at extremely low dynamic pressures. The latter system includes a series of jets located at the wing tips and in the nose of the fuselage to give pitch, roll and yaw control. All controls, wiring and plumbing are contained within a side fairing extending nearly the



Figure 1. The X-15.

full length of the fuselage. The aircraft is not designed for normal ground take-off, but is carried aloft by a suitably modified B-52 bomber. Suspension is from a special pylon located under the right wing of the bomber. The aircraft is powered by a single XLR99-RM-1 rocket engine, with throttling capability, which uses anhydrous ammonia and liquid oxygen as fuel. Auxiliary power is derived from turbines using hydrogen peroxide. Heat resistant nickel base alloys are used for most of the structure, especially the exterior surface. The cockpit enclosure is jettisonable in flight as well as the pilot's seat with pilot.

The internal arrangement is such that the lifting surfaces serve only their primary purpose with all installations contained in the fuselage and side ducts. The nose compartment of the fuselage contains an instrument bay, nose wheel, and ballistic control nozzles. The cabin section follows containing the pilot, controls, and necessary appurtenances. Immediately aft of the cabin is a compartment containing environmental equipment, systems instrumentation, and auxiliary power. Behind this section lie the integral propellant tanks containing LOX and NH₃, in that order. In the tail

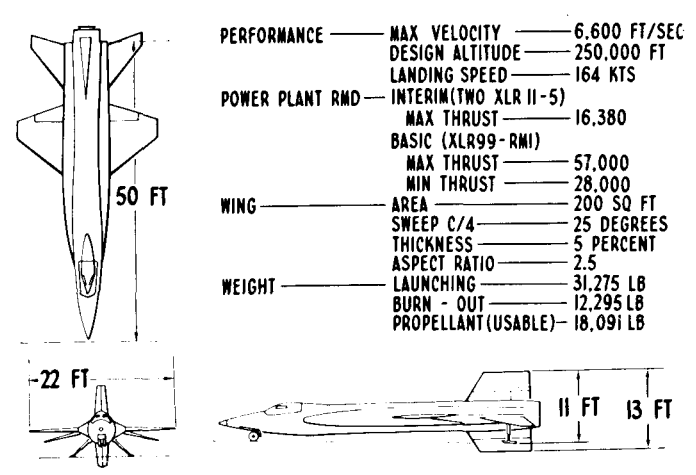


Figure 2. Three view.

section is located the rocket engine complete with auxiliaries, the main landing gear, horizontal and vertical tail surfaces. A part of the lower vertical tail is jettisoned just before landing and is recovered by means of a parachute. This is an essential feature since the lower vertical tail extends below the landing skids in their extended position. All landings are planned to be made on Rogers dry lake bed in California but may be made on several of the dry lake beds found in the western part of the U.S.A. The entire vehicle is finished with a heat resistant paint. A perspective view of the aircraft showing the general arrangement is shown in Fig. 3.

The design requirements for the X-15 are summarised as follows:

Maximum Velocity—6600 feet per second.

Altitude Capability—250 000 feet minimum.

Representative primary structure should experience a temperature of 1200 degrees F. (650°C).

Portions of the structure should achieve a heating rate of 30 btu per square foot per second.

Purpose: to enable the study of problems pertaining to hypersonic flight by means of manned aircraft.

Up to the present time, the three aircraft collectively have practically attained or exceeded all of the design requirements. New records in both speed and altitude have been achieved. On 27th June 1962, NASA pilot Joseph Walker attained a speed of 4159 miles per hour at a Mach number of 6.09. A few days later, on 17th July 1962, Major Robert White, U.S.A.F., piloted another X-15 to an altitude of 314.750 feet

(59.6 miles) which is well beyond the earth's atmosphere. By the beginning of 1963, more than 75 powered flights have been made by the seven pilots assigned to this project. The total number of flights is almost evenly divided between those made with the interim XLR11 engine and those with the more powerful XLR99. The flights with the large engine, with a few exceptions, were all made at a Mach number greater than 4.0 and, of these, the majority have well exceeded 5.0. Altitudes above 100 000 ft are nearly always attained, depending on the mission, and excursions above 200 000 ft have been made on several occasions. Thus, the performance has been most satisfactory and with continued care in executing the many flight test programmes that are planned, a wealth of knowledge will result.

Materials

STRUCTURAL

The materials used in the X-15 were selected on the basis of their compatibility with strength, temperature environment, corrosion resistance, and processing requirements. It was obvious from the start that much of the wetted surface would be subjected to temperatures of 800-1200°F and would require high strength at these temperatures. Exotic materials utilising the rare elements had not advanced to quantity production or usage and consequently the list of possible candidates narrowed to the corrosion resistant steels, titanium, and nickel base alloys. Fig. 4 shows a comparison of the contending materials with a high strength aluminium alloy added for interest.

The familiar strength/density ratio is used in three of the plots shown since it portrays a measure of structural efficiency. It will be noted that whereas 6Al-4V titanium and 350 CRES show higher strength efficiencies over a wide temperature range, each falls off rapidly above 800°F while Inconel X shows only a gradual drop in strength up to 1200°F. Because of this stability, Inconel X was selected for the skin covering for the entire air vehicle. Also of interest, where structural stiffness is required, the plot of modulus/density against temperature shows Inconel X to have the advantage in the 800-1200°F range. The non-heat-treatable but weldable Inconel was used in those locations where high strength was not paramount and where final close-out welds were necessary following heat-treatment of the surrounding structures. Thus, Inconel lands were incorporated in the Inconel X structure before final heat-treatment. Access hole cover plates made from Inconel were finally welded to these lands.

The internal structure was made from a variety of materials in consonance with the environment. High strength aluminium alloy (2024-T4) was used to form the inner pressure shell

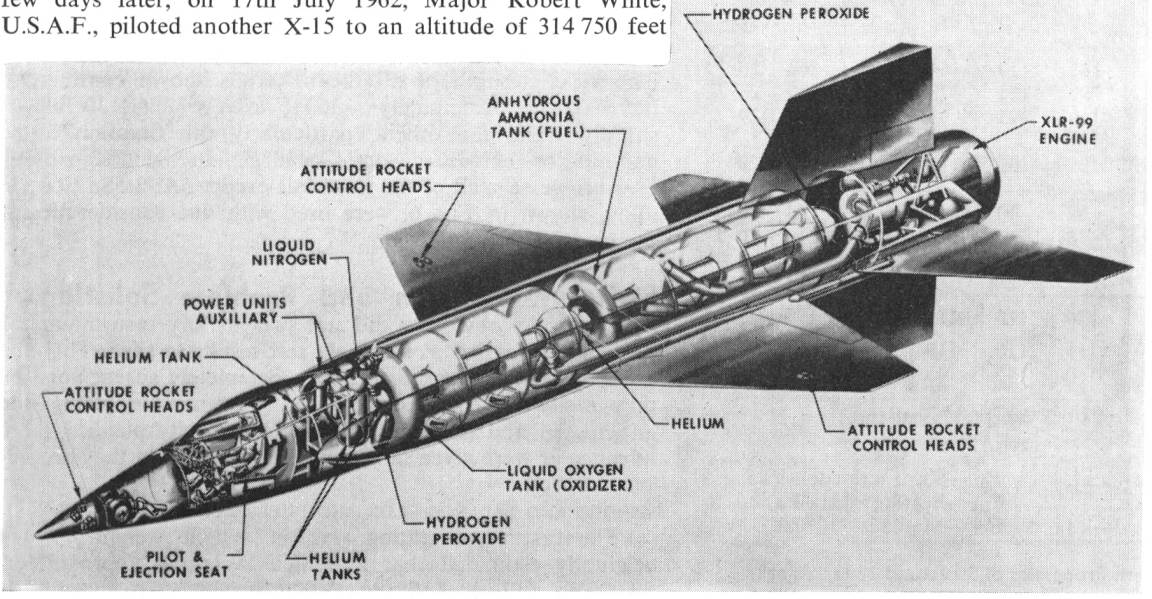
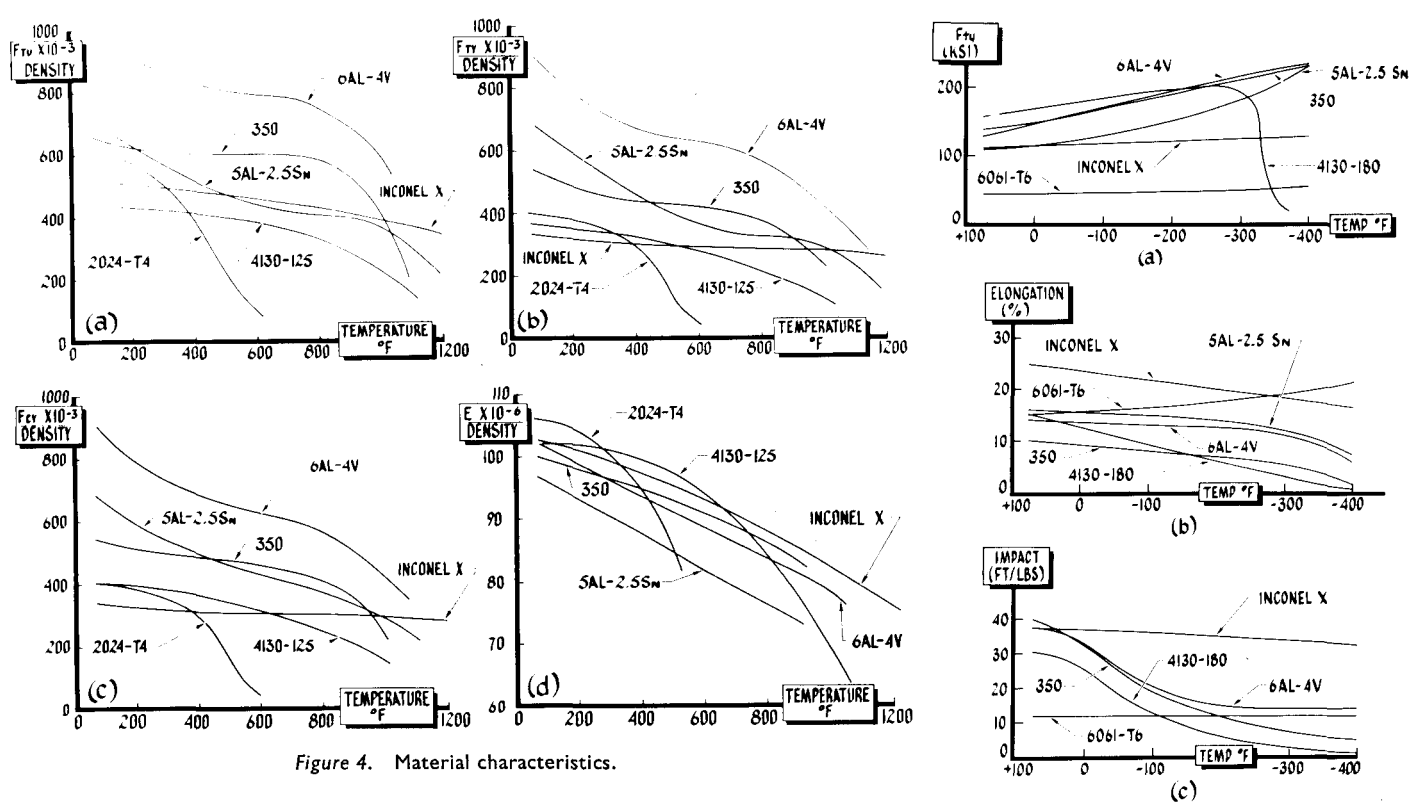


Figure 3.
General arrangement.



of the cockpit and part of the equipment bay. As a relief from high thermal stresses in the internal structure of the lifting surfaces and fuselage, titanium alloys were used. These originally were of two compositions; namely, 8 Mn titanium which was the highest strength alloy then available but not recommended for welding and 5Al-2·5Sn which had good strength and was weldable. Later, a higher strength and weldable titanium alloy (6Al-4V) was introduced. Titanium framing was used almost exclusively in the aft fuselage structure where high concentrated loads are to be found. The most commonly used structural materials and their properties

Material F_{TY} F_{CY} \boldsymbol{E} $F_{
m SU}$ F_{TU} F_{BY} *Inconel X 100 Nickel 155 105 108 186 31 Inconel base 80 30 32 56 31 *350 Cres 185 150 125 28.7 164 268 Steel *355 Cres 200 165 178 131 295 28.7 *A-286 Cres 140 95 99 91 136 29 4130 (HT125-Mo) 125 103 82 29 113 180 Aluminium *2024-T4 62 40 40 37 10.5 *7075-T6 alloy 78 69 70 47 110 10.3 *6061-T6 35 42 36 27 58 10.2 $8 M_N$ 79 120 110 115 180 15.5 5Al-2.5S_N 110 Titanium 115 110 72 175 15.5 6Al-4V 160 145 145 99 230 16.3

Properties are for bare sheet stock except 355 bar stock *heat treated

 F_{TU} —Tensile ultimate—k.s.i. F_{TY} —Tensile yield—k.s.i. F_{CY} —Compressive yield—k.s.i.

F_{SU}—Shear ultimate—k.s.i. F_{BY}—Bearing yield—k.s.i. E —Modulus—10⁶ p.s.i.

Figure 5. Strength Properties of Structural Materials at Room Temperature.

Figure 6. Material properties at low temperature.

are listed in the table of Fig. 5. Fusion welding was used predominately throughout the construction but always in a controlled atmosphere. Resistance welding was also used. All critical welds were radiographically inspected to assure high quality and soundness.

PRESSURE VESSELS

The materials used in the many pressure vessels had to be selected not only on the basis of strength but ductility as well. Fig. 6 shows significant properties of several materials at low temperatures. Martensitic alloys, such as heat-treated 4130 low alloy and 350 precipitation hardening corrosion resistant steels, exhibit a considerable loss in ductility as the temperature continues to decrease to large negative values. It will be noted that Inconel X, the two weldable titanium alloys and 6061-T6 show more favourable characteristics in this respect. The yield strength of all the materials shown continues to increase to approximately -300°F after which 4130 falls off sharply while the others, particularly the titanium alloys, continue to increase beyond -400° F. In the design of the pressure vessels, all of the materials except 5Al-2.5Sn titanium alloy, shown in Fig. 6, were used with due consideration of the environment involved.

Structural Design and Problem Solution

The X-15 obviously did not present any insurmountable problems in design as the flight test results testify. This does not mean that new problems were completely absent nor were they easily solved. Nevertheless, most new problems were anticipated and their solutions were carefully planned far in advance or were given immediate attention when they arose.

WEIGHT AND BALANCE—LOX AND FUEL FEED SYSTEM

The first consideration was air vehicle weight. It was originally estimated that a vehicle weighing approximately 30 000 lb, fully loaded and 12 000 lb without fuel, would be

Item	Specification weight lb.			
Weight empty				
Wing	1406			
Empennage	1078			
Body group	3812			
Alighting gear	447			
Surface controls	937			
Propulsion Group—Engine	540			
—Propulsion systems	868			
Auxiliary powerplant group	270			
Fixed-equipment group	1216			
Instrumentation	800			
Total weight empty	11374			
Useful load				
Pilot	290			
Oxidiser (engine lox)	10080			
Fuel				
NH ₃ (engine)	8011			
H ₂ O ₂ (engine pumps)	889			
H ₂ O ₂ (APU and ballastic control				
systems)	268			
Trapped oil, fuel, and oxidiser	82			
Helium	49			
Nitrogen (Cockpit pressure and cooling)	232			
Total useful load	19901			
Total gross weight	31275			
Weight at burn-out	12295			
Landing weight	11946			

Figure 7. X-15 Weight statement.

required to perform the missions prescribed. After the basic configuration was agreed upon, a vehicle design estimated at 31 275 lb emerged, which included nine tons of fuel and oxidiser. Upon completion, the airframe was approximately 400 lb heavier than the specification weights shown in Fig. 7.

A foreseeable problem developed in maintaining the proper balance of the aircraft. Expending nine tons of propellants in a matter of seconds, and maintaining a nearly constant centre of gravity location required immediate consideration. The LOX tank containing approximately 1000 gallons was located forward and the ammonia tank with 1400 gallons was located aft of the centre of gravity. Each tank was divided by semi-torus frames into three compartments. The seven cubic feet of helium gas at 3600 psi pressure had almost negligible weight and was located forward. Control was established by expelling the LOX and ammonia towards the centre of gravity location, that is the LOX was expelled aft through the tank

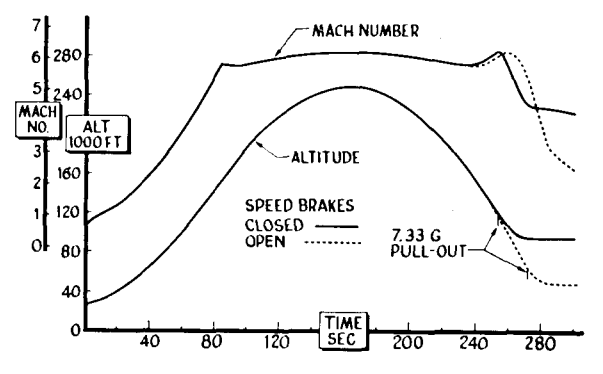


Figure 8. Design altitude mission.

compartments whereas the ammonia expelled forward in the same manner. In this way, the movement of the centre of gravity during powered flight was held to $3\frac{1}{2}$ per cent. No other weight or balance problem developed which required special considerations. Like most aircraft that have seen service, miscellaneous variations in equipment and minor changes have resulted in some flights being made at weights approximating 33 800 pounds.

AIR LOADS

Since the mission of the X-15 was manned flights at extremely high speeds, altitudes, and temperatures, the design criteria centred around basic missions such as shown in Figs. 8 and 9. The first mission was based on flight at 250 000 ft altitude and a velocity of 6300 feet per second. Two types of pull-outs were considered—each maintaining a zero lift trajectory until time of pull-out. One type of re-entry uses a maximum angle of attack entry wherein the speed brakes remain closed and pull-out is initiated at a predetermined altitude which is the highest where available lift and control power permits a 7.33g manoeuvre. In other types of re-entry, the speed brakes are deployed at the peak altitude and a 7.33g recovery is initiated at a point so as not to exceed a limit dynamic pressure of 2500 pounds per square foot. To attain a true airspeed of 6600 feet per second, the pull-up after launch is made to a lower climb angle than for the altitude mission. The design speed is reached at burn-out, from which a zero lift coast is made to approximately 130 000 feet. From this altitude, recoveries similar to the high altitude missions are made.

To provide a reasonable strength level, the aircraft was designed for limit manoeuvre load factors of 4.0g and -2.0g before burn-out and 7.33g and -3g after burn-out. Although the maximum product of load factor and weight (nW) occur during exit, the re-entry condition at high temperature is generally more critical. The limiting dynamic pressure of 2500 pounds per square foot was chosen as representing reentry at the lowest altitude for recovery consistent with safety for terrain clearance. This dynamic pressure is reached at an altitude of 40 000 feet during a pull-out at Mach 3.0. Below this altitude a maximum dynamic pressure of 1600 pounds per square foot was used.

In order to avoid an unnecessary weight penalty, the pullout at 7.33g at maximum dynamic presure should only be attained once during a particular recovery. During this manoeuvre, the aircraft slows down appreciably and heats up rapidly. If another pull-up is required following the first, it must be made at a lower acceleration to avoid overloading the heated structure.

A comparison of wing chordwise pressure distributions may be of interest and is shown in Fig. 10. The upper curve is for a pull-out at high dynamic pressure and low supersonic

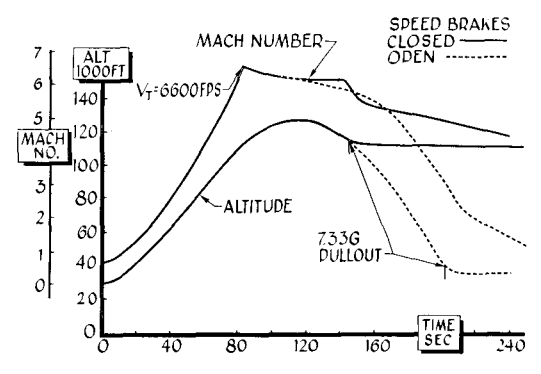
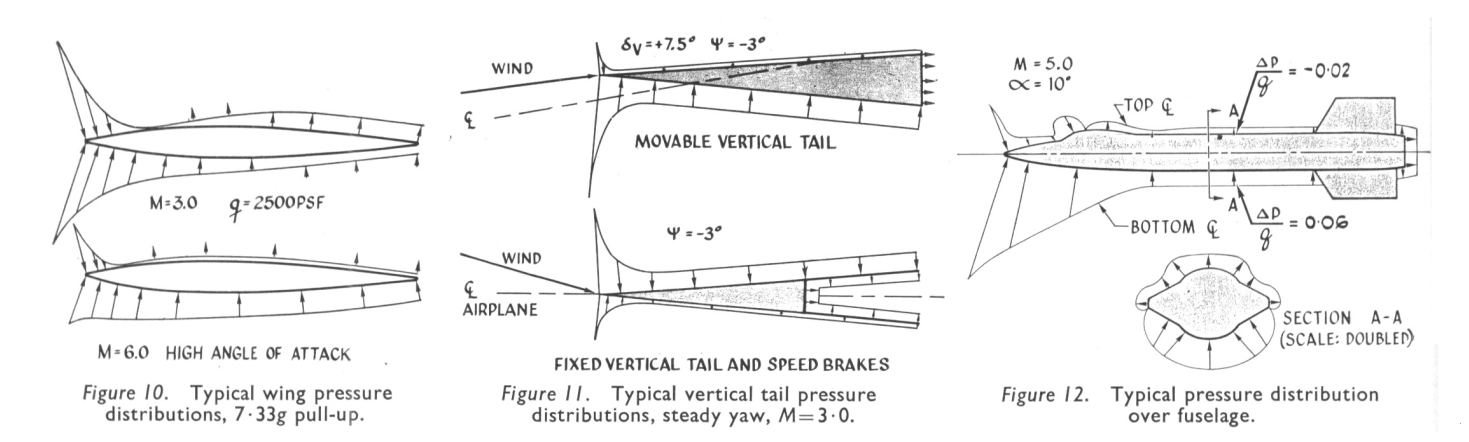


Figure 9. Design speed mission.



Mach number. The other is for a pull-up at both a high Mach number and angle of attack. Pressure distributions for the horizontal tail are similar to the wing. The pressure distributions over the vertical tail are unique both for the allmovable portion and that containing the speed brakes. Typical distributions are shown in Fig. 11.

The pressure distributions in the plane of symmetry over the fuselage are shown in Fig. 12. The effect of the cockpit canopy is clearly seen. In the moderate angle of attack range (0-10 degrees) the body carries approximately 45 per cent of the total wing-body load and this increases to 65 per cent at 20 degrees angle of attack. Thus during a 7.33g recovery when inertia loads are high, the large air loads support the fuselage along its entire length.

An apparent air load problem was anticipated during the launch phase with the X-15 suspended under the wing of a B-52 bomber. This installation was similar to suspending a large finned external fuel tank or store on any other aircraft. However, in size and weight, there was no comparison. After a careful review of all factors affecting this operation, it was determined that the following level of strength would be adequate: strength to permit control system checkout of the X-15 still attached with full surface deflection up to a maximum equivalent airspeed of 300 knots. Prior to drop, a manoeuvre restriction to 1.6g would suffice. The latter also provided sufficient strength for gust intensities of 30 feet per second at speeds up to 300 knots. Since all flights are carefully controlled, operations in thunderstorm activity and clear air turbulence are easily avoided. So far no load problems have developed as a result of this "pigga-back" operation.

A typical design mission showing load against temperature is shown in Fig. 13. It will be noted that a reasonably high normal acceleration (approximately 3.5g) is reached during the initial climb but all temperatures are in the frigid region. The weight at this stage is slightly less than maximum—being

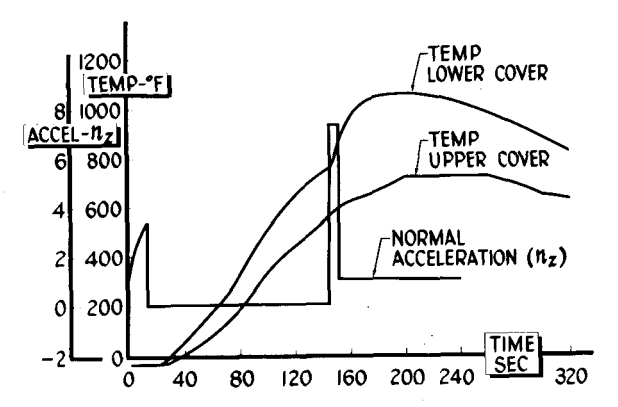
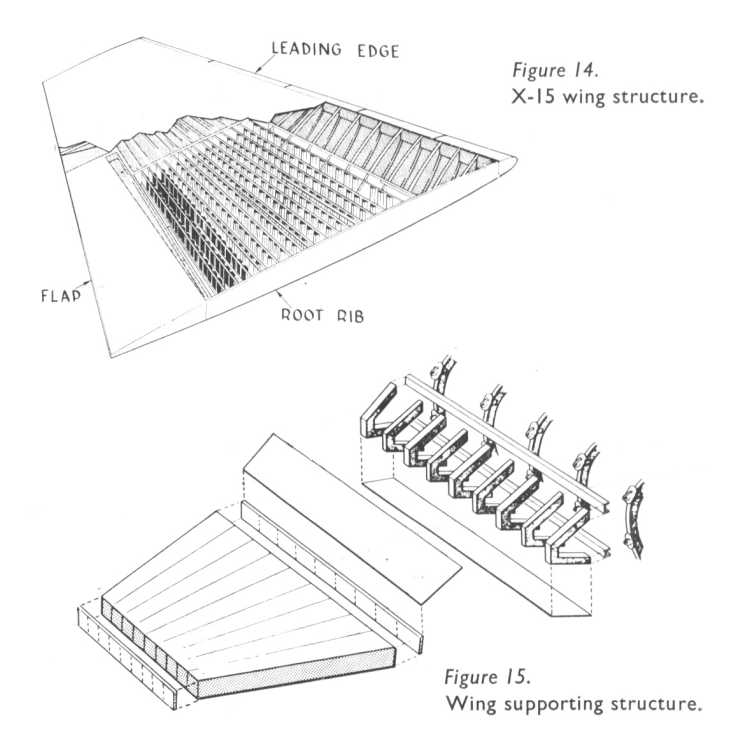


Figure 13. Temperature plotted against load, high-speed mission.

approximately 26 600 pounds. During re-entry before peak temperatures on the wing are attained, a pull-out manoeuvre at maximum normal acceleration is executed. The maximum load stresses therefore precede the maximum thermal stresses. This schedule of stresses was an important factor in the design.

WING DESIGN

Figure 14 presents a sketch of the wing outer panel which is a multispar box beam design. The skins are unreinforced Inconel X sheet because of its strength and favourable creep characteristics at 1200°F. The skin thickness varies from 0.090 inches at the root to 0.040 inches at the tip for the upper surfaces and 0.065-0.40 respectively for the lower surface. The internal structure is built entirely of titanium alloy sheet and extrusions. Both the front and rear spars consist of flat web channel sections. The intermediate spars have corrugated webs which are attached to the skin through separate angles. The three ribs used in the design are of the same construction as the front and rear spars. Attachment of the above is by means of A-286 rivets and screws. The leading and trailing edges, however, are of multi-rib design where panel size was determined by stiffness requirements. The extreme leading edge itself consisted of a solid bar of Inconel X which acts as a heat sink. The Inconel X leading



edge was originally divided into five segments to minimise thermal stresses. Following a very hot flight there was some evidence of local inter-rivet buckling adjacent to the slot and the number of segments was increased to nine.

The details of the wing to fuselage attachment are shown in Fig. 15.

The redundancy of support is clearly indicated and the solution of an involved elastic analysis was necessary to obtain the proper load distribution. The outer panel attaches to the side tunnel through nine "A" frames which redistribute their loads through the cover panels to the five carry-through frames. Thermal gradients of 400 to 500°F are possible in this region up to burn-out because of the low temperature of the LOX (-320°F) contained in the plumbing in the side fairing.

The temperature profiles shown in Fig. 16 reflect the peak values for the critical thermal mission which occurs during re-entry of the vehicles into the atmosphere. The maximum values occur at the stagnation and adjacent points. The temperature differential between the upper and lower surfaces is shown in this figure to be approximately 400°F. The surface gradients existing in the structural box are of tolerable magnitude. This is the case both spanwise and chordwise.

Profiles of thermal gradients at the critical instant are presented for three typical sections of the wing in Fig. 17. The steepest gradient between the skin and centre of the spar web is 900°F. Laboratory tests reflecting gradients of this magnitude did not indicate any obvious adverse effects.

To arrive at a near optimum in design, a structural efficiency analysis was made of the wing at three representative sections: inboard, intermediate, and outboard—at room temperature. Minimum structural weight is shown in Fig. 18 as a function of the design variables of bending moment, wing chord, wing depth, and skin-cover thickness. The variables are presented in index form. The points of the wing plotted in the graph in this figure indicate an essentially optimum balance of the parameters in question as all of the subject points lie close to the maximum efficiency curve.

Figure 19 presents a comparison of the thermally induced skin and spar-cap stresses due to a temperature gradient for two different material combinations. This comparison reveals the superiority of the Inconel X skin and titanium spar-cap combination to one of all Inconel X. The thermal stresses are definitely lower for the Inconel X skin and titanium combination, which is also lighter in weight.

The wing stress analysis involved both simple beam theory as well as the solution of the redundant root structure. Outboard of Station 89 (approximately mid-span), a simple cantilever eight cell beam solution was sufficient to determine load stresses. Inboard of Station 89 the wing is partitioned into nine individual box beams and a single cell torque box to which were applied the redundant shears and moments from the structure surrounding the root rib. The solution of the internal loads in the wing at the root section involved 33 redundants and was programmed on an IBM 704 type computer. The fuselage attachment assembly was bi-metallic with Inconel X wing and side fairing covers and titanium alloy (5A1-2.5Sn) forgings and extrusions forming the "A" frame details. The stiffness of each was proportional to its respective modulus of elasticity or secant modulus depending on stress levels. Thermal stresses in the wing were calculated and added to the load stresses in the elastic range. The classical assumption for beam theory was included; namely, that plane sections remain plane under thermal stresses. Throughout the design of the wing, many artifices such as beads, lightening holes, scallops, and corrugated webs greatly minimised internal loads from thermal strains.

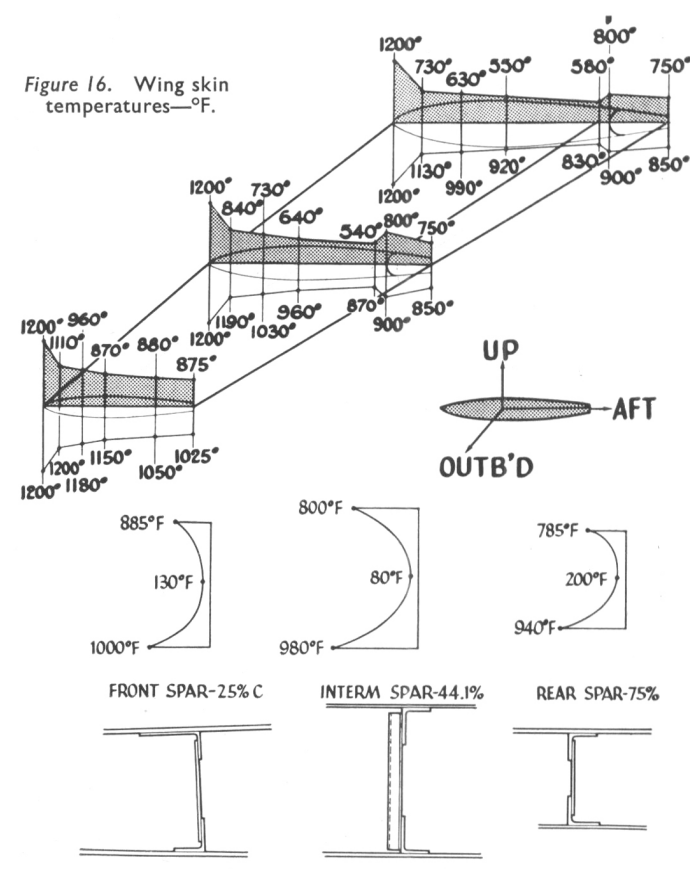


Figure 17. Wing temperature gradients.

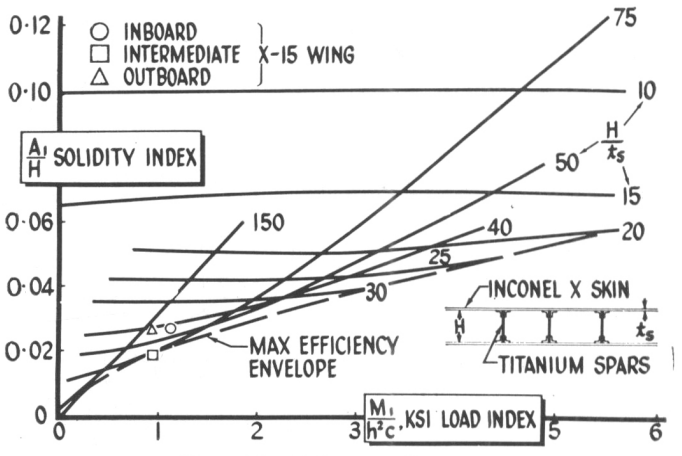
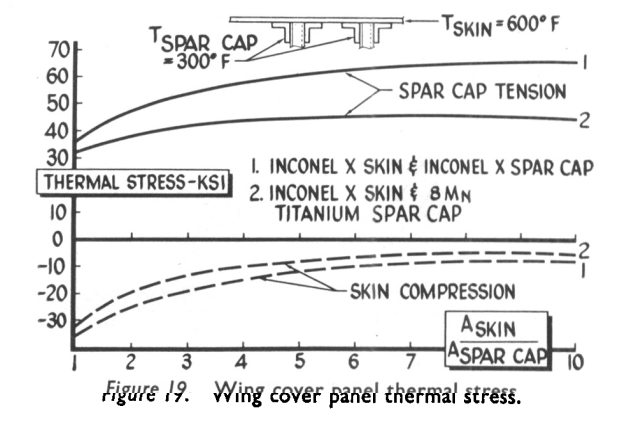


Figure 18. Multi-spar efficiency.



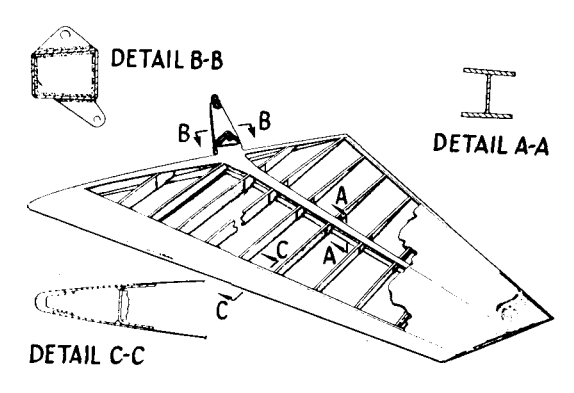


Figure 20. Horizontal stabiliser.

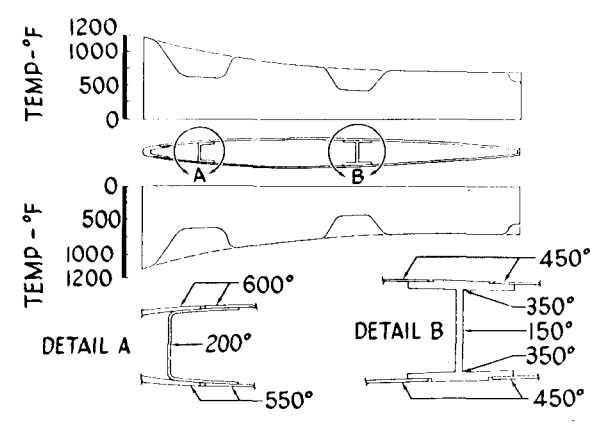


Figure 21. Horizontal stabiliser temperatures.

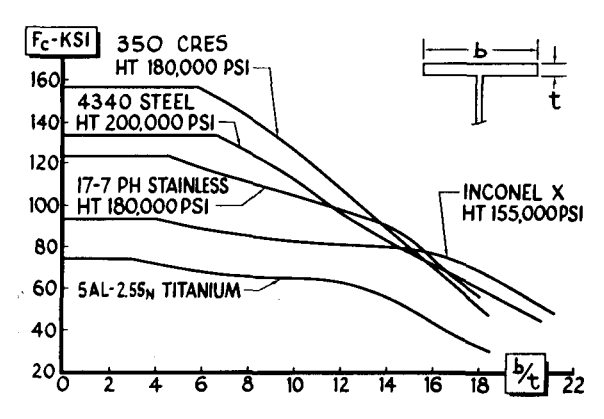


Figure 22. Spar-cap allowable stresses at 500°F.

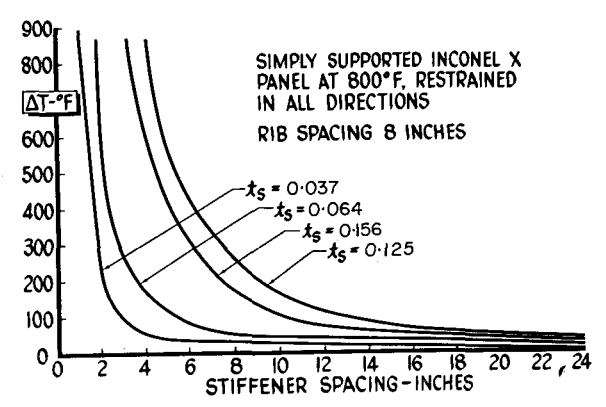


Figure 23. Critical temperature differential for buckling.

HORIZONTAL STABILISER DESIGN

The horizontal stabiliser structure is shown in Fig. 20. The left- and right-hand stabilisers are mounted separately and thus provide both lateral and longitudinal control for the aeroplane. The structure consists of an Inconel X main spar, an A-286 front spar, a titanium trailing edge, Inconel X ribs ahead of and 8 Mn titanium ribs aft of the main spar, and 0.050 in Inconel X skin. The surface is all-movable about a spindle which is an integral part of the main spar and which attaches to the fuselage in the region of the side tunnels. For the most efficient design, the main spar is used to carry all normal bending along the entire span. The front spar effectively closes out the torque box which terminates at the root rib. Actuation is by an hydraulic cylinder attached to an arm located in line with the outboard bearing.

Figure 21 shows the maximum skin temperatures on the horizontal tail and also gives the maximum temperature gradient between the skin and the spar-caps. The distribution is given for a station at mid-span and is typical since the skin gauge does not taper spanwise or chordwise, with the exception of the nose skin forward of the leading-edge beam. The temperature of the nose skin is controlled to a maximum value of 1200°F by varying the thickness between the leading edge and front spar. The decrease in temperature in the area of the beams is due to the large mass of the beam caps with respect to the thin skin.

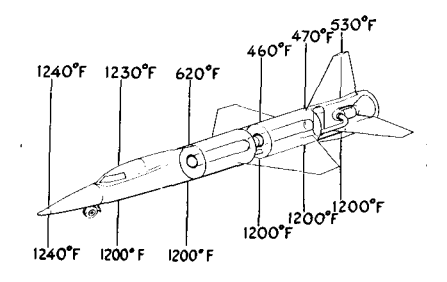
Allowable stresses for various materials at 500°F were calculated to determine the optimum spar-cap material and the results are presented in Fig. 22. At a b/t of 10, 350 CRES steel shows an advantage over all other applicable materials. The advantage of strength, however, was not of prime importance in this case. The resulting thermal stresses produced early skin buckling and so reduced torsional stiffness that Inconel X was chosen for the main spar.

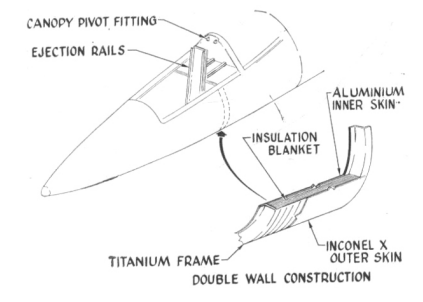
A study was made in consideration of the problem of whether to permit the stabiliser skins to buckle under elevated temperatures. The curves shown in Fig. 23 give the allowable temperature differential between the skin and internal structure for initial buckling of Inconel X panels heated to 800°F and include various skin gauges and spanwise stiffener spacing with a constant 8-in rib spacing. It was assumed that the panels were restrained in all directions by virtue of the elastic properties of the skin and stiffeners.

It was found that for even small temperature differences, it is necessary to increase the skin gauge and decrease the stiffener spacing in order to eliminate skin buckling. This would impose severe weight penalties. For example, to increase and stiffen the skin to prevent buckling up to limit conditions would add 195 pounds. Consequently, thermal stress buckles were permitted to exist during the brief period of heating at the re-entry, but no permanent buckles were condoned. A skin thickness of 0.050 was finally selected with no stiffeners.

VERTICAL TAIL SURFACES

The vertical tail surfaces extend above and below the fuselage. Each portion contains a fixed structure which is integral with the fuselage and supports a pair of split trailingedge speed brakes. The cross section of each vertical surface is wedge-shaped for best aerodynamic performance. The fixed box structure is a mixture of Inconel X and titanium alloy with Inconel X skin-covering. The speed brakes are hinged from the fixed portions and each pair is actuated by an hydraulic strut. The brakes utilise Inconel X skin covering reinforced by a corrugated inner skin and ribs made of the same material. Above the upper fixed structure is an allmovable section made entirely of Inconel X and employs front, main, and rear beams. The main and rear beams plus





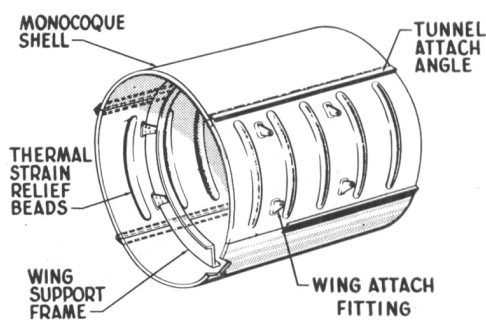


Figure 24. Fuselage design temperatures.

Figure 25. Fuselage skin.

Figure 26. Fuselage main shell.

skin form a box beam for attachment to the fixed portion. A spindle support having two bearings spaced 18 inches on centre completes the attachment. An hydraulic strut is used to actuate the all-movable portion of the surface. The section of the lower vertical surface below the fixed portion is jettisonable. While attached, it is all-movable as in the case of its counterpart in the upper portion above the fuselage. Release of this section is by means of explosive bolts and, after release, a parachute is deployed to lower it to the ground for use in another flight. The type of construction in the jettisonable section is the same as the all-movable part of the upper surface.

FUSELAGE DESIGN

The fuselage structure is divided into three distinct sections as far as structural design is concerned. Fig. 24 shows the temperature distribution along the fuselage through the plane of symmetry. The forward section extending from the nose to the forward end of the LOX tank is semi-monocoque. The region surrounding the cockpit and parts of the equipment bay utilises a double wall construction. The outer skin is Inconel X and the inner wall is 2024 T4 aluminium alloy with spun glass matting for insulation in between. The inner wall is only used as a pressure seal and is so designed. The intercostals connecting the inner and outer skins are titanium alloy. The double-walled construction is shown in Fig. 25. Since the nose wheel is located far forward in this part of the fuselage, the whole forward section was designed chiefly by landing and ground handling conditions.

The centre-section of the fuselage forms the propellant and oxidiser tanks. Since no insulation is used, a pure monocoque structure resulted. This portion of the fuselage was designed by critical conditions from both flight and landing conditions. The monocoque construction obviously simplified the design to a very large extent and eliminated many of the thermal stress problems that might have resulted from a more complex configuration. Provisions were made, however, to relieve thermal stresses in the side duct areas by using partial circumferential beads in the skins.

The weight penalty to operate an air vehicle at high aerodynamic heating is high. The thickness of the shell required to keep materials, other than Inconel X, within their maximum allowable temperature would cause the weight of the shell to exceed greatly that using Inconel X. Actually, the choice of optimum material depends on the magnitude of the applied loads. If the loads are heavy, then the mass of the structure will easily absorb the heat input with only a small temperature rise. This would permit use of an efficient low-temperature structure. However, when the loads are relatively light and the heat input is large, as in the X-15, minimum weight is obtained by using a high-temperature resistant material.

The fuselage basic structure through the propellant tanks is shown in Fig. 26. For a given heat input and material,

there is a minimum skin thickness which results in a heat rise sufficient to weaken the material beyond practical use. This would necessitate heavy skins if semi-monocoque construction were used. Hence, with only a slight increase in skin thickness, monocoque construction is possible. This had many advantages—the first of which was minimising thermal stresses. Since all of the structural material was on the surface, all of the material has an equal opportunity to be heated and the temperature gradient quickly approaches unity. The circular cross-section was ideal for service as a pressure vessel. Due to the relatively low stresses developed, skin billowing was eliminated and fatigue and creep problems were minimised. The thick skin material also helped both in fabricating the fuselage and sealing the tanks.

The semi-torus bulkheads offer a minimum of radial restraint to the monocoque shell under a thermal gradient since they are attached tangentially. The tests that were performed on a section of the fuselage through the main tank region verified all the points made difficult because of the temperature involved. The presence of the side ducts, however, shrouded those portions over the fuselage and thus shielded it from high aerodynamic heating. The resulting thermal strains in the upper and lower portions of the tank structure would have buckled the side skin longitudinally at a temperature differential as low as 300°F. To eliminate this condition, the side skins were beaded vertically in the vicinity of the side ducts, but some compromise was necessary since the stresses, due to tank pressurisation, had to be shunted around these regions. The stress analysis assumptions were completely verified by the structural tests that followed.

A typical arrangement of the structure in the propellant tanks is shown in Fig. 27. The material chosen had to be weldable for sealing purposes. Each tank was divided into three compartments and each compartment farthest from the aeroplane c.g. contained longitudinal baffles. The assembly procedure required building all plumbing in each compartment in turn before completing the next compartment.

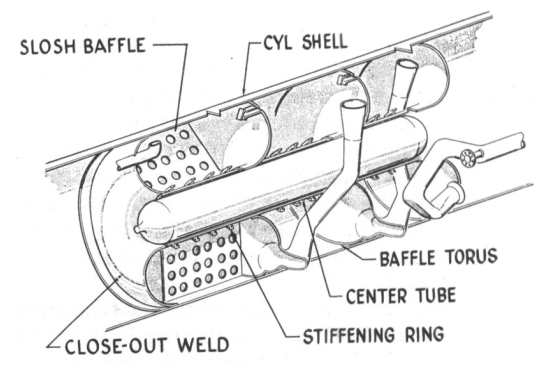


Figure 27. Liquid oxygen tanks.

The side ducts were at first designed as continuous throughout their length. After several hot flights, some residual buckles developed which required attention. Accordingly, several expansion joints were incorporated in the side ducts of all three vehicles.

The aft section of the fuselage was designed as a semimonocoque structure along more conventional lines. The outer skin made from Inconel X was riveted to heavy titanium framing. The latter was arranged to accommodate high concentrated loads introduced by the engine mount, landing gear, and empennage attachments. The design of this portion of the fuselage offered no particularly difficult problems.

The fuselage stress analysis became considerably more involved due to the redundant nature of the reinforced shell structure and the transition to pressurised tank sections in between. It became necessary to depart from the more conventional engineering beam treatment. The application of the principle of minimum strain energy resulted in a solution that accounted for such features as tapered webs, longerons and stringers, frame bending, and shear lag effects. The effects of discontinuities such as cut-outs and end restraints could also be included in this type of analysis if such details were desired.

An IBM programme was prepared to help in the solution for all the redundants included in the analysis. The programme had a capacity for 70 internal redundants which permitted the solution of a fair size section of the fuselage at one time. An interlocking programme also limited to 70 redundants enabled the solution of joined sections. The effective structure had to be selected with care and sections and lengths chosen so as to reflect rapid or abrupt changes in structural arrangement. Frame energies were also included in the general solution. Thermal stresses were computed for all important members, particularly frames.

The oxidiser or LOX tank section of the fuselage was first analysed for an internal pressure of 111 psi ultimate. Next it was analysed for critical external loads which included the normal array of shear, axial, bending, and torsional loadings. A third case arose in designing the tank section for a negative or collapsing pressure reaching a maximum of 6 psi ultimate. The high load carrying sectors, namely, the upper and lower Inconel X segments had a thickness of 0.063 which was stiffened by light welded on "J" section ring frames with an area of 0.0355 square inches and an average spacing of 6 inches. The allowable buckling stresses were determined from tests of curved panels with due consideration to their post buckling strength. The maximum temperature in the LOX tank at the inner torus and cylinder is 307°F and the minimum temperature when filled is -320°F. Both temperatures, however, do not occur simultaneously. The LOX tank is also subjected to fore and aft inertia loading from the contents. Since the inner tori frames are not designed to carry bending, the fore and aft LOX loads are transferred to the outer shell wall by means of three radial flat panels acting as baffles. The baffles, in turn, are supported from the inner shell wall and hence deliver only a shear loading into the outer shell. The inner shell referred to above supports the cylindrical helium storage bottle as well as the tori bulkheads, and adds to the general stiffness of the tank assembly. The inner shell must also resist collapsing due to the high main tank pressure. During the design of the tank structures, careful attention was paid to the various piercing of hardware and plumbing items. Vibratory loads were considered for all important attachments.

The design and analysis of the ammonia tank portion of the fuselage followed closely its counterpart in the LOX tank. The maximum pressure inside the ammonia tank was the same as for the LOX tank but the minimum temperature was

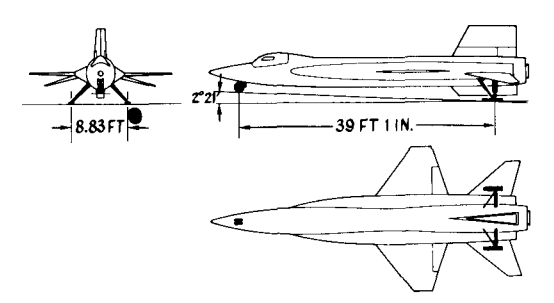


Figure 28. X-15 landing gear.

 -24° F. The inner shell, however, is filled with fuel instead of serving as a container for a gas storage bottle as was the case for the LOX tank.

LANDING GEAR DESIGN

The unique landing gear configuration (Fig. 28) adequately fulfilled the requirements for this aeroplane. The extremely far aft location of the main gear was made possible by the fact that since the X-15 is air-launched, the usual nose wheel lift-off requiring rotation about the main gear was not necessary. All gears are retracted manually while the aeroplane is suspended from the B-52 and are free falling upon release with air drag assisting. The main gear skids are pinned in two planes to permit pitch and roll but are restrained in yaw. Co-rotating nose wheels are used to prevent shimmy and to offer less castoring torque resistance than an hydraulic damper. This is an important consideration since excessive castoring friction and damping can cause directional instability.

The design requirements for the landing gear included (a) sinking velocity 9 feet per second, (b) landing speeds at touchdown from 164–200 knots, (c) aeroplane attitude of 6 degrees included ground angle.

With the gear arrangement just described, a normal landing loads computation was not considered applicable. A dynamic analysis was made wherein the gear reaction, aerodynamic forces and moments, and resulting aeroplane motions were computed as a function of time. As might be expected, the nose gear reaction was unusually high, reaching values 50 per cent greater than the combined main gear loads. A time history of a high sink speed landing is shown in Fig. 29. The vertical velocity of the nose wheel increases from its initial value of 9 feet per second at the time of main gear contact, to 18 feet per second at its point of contact. The resulting nose gear acceleration reaches a value of 3.9. It will be noted that the aeroplane attitude at touch-down is an important control-

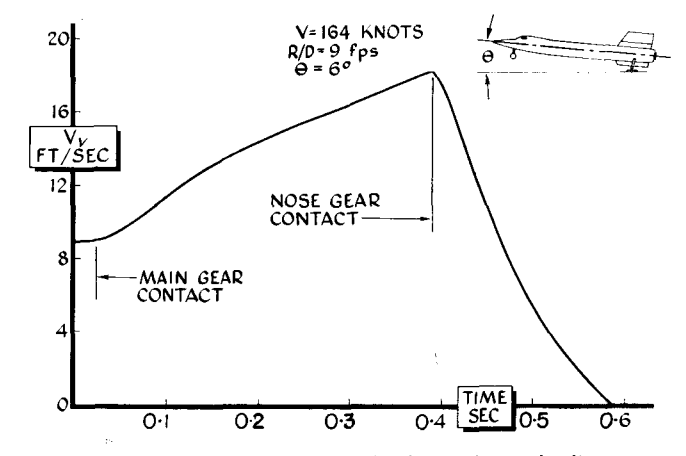


Figure 29. Nose gear vertical velocity during landing.

ling factor. Therefore, high speed landings are usually made in excess of 164 knots.

Three test programmes, other than the dynamic drop tests of the shock absorbers, were executed in the development of the landing gear. These included a dynamic model test for stability, a nose wheel shimmy test, and full scale main gear skid tests on the dry lake bed used for landing. A one-tenth dynamic model was built with a 360° free swivelling nose wheel having co-rotating rubber tyres. Provisions were made for two main gear locations—one in the tail and one near the centre of gravity. The tests, however, favoured the location in the aft section of the fuselage. The model was catapulted by a rubber shock cord along a concrete runway and overhead cameras recorded yawing oscillations during each run. After several convergent oscillations, the model ran straight for a scale distance equivalent to an aeroplane run-out of 6000 feet. The model nose wheel had provisions for varying the spindle friction and this permitted the establishment of a maximum permissible torque of 130 foot pounds. The actual torque friction in the aeroplane is approximately one third of this value. In this way the landing stability was established at an early period in the design.

Full scale nose wheel shimmy tests were later conducted at the NASA landing test facility at Langley Field, Virginia. These tests explored a velocity range from 20–125 mph and conditions representing wet pavements, sand, uneven tyre pressures, one flat tyre, and unbalanced wheels. Blocks placed in the path of the nose wheel were used to induce shimmy. These tests proved that neither shimmy dampers nor torque links were needed.

Tests using a pair of full scale main skids were made on the dry lake bed. The skids were mounted on a retractable carriage fastened to a trailer and drawn by a truck (Fig. 30). Speeds up to 70 mph were attained with this test rig. When the test speed was reached, an electrically operated release dropped the skids on to the lake bed and high speed cameras recorded the motions. Other instrumentation recorded the vertical and drag loads, strut stroke, etc. From the recorded data, the coefficient of friction of the landing surface was determined. "Landings" were also made on a concrete surface as well as the lake bed. Friction coefficients obtained for landings on the lake varied from 0.35 at high speed to 0.8 at the point of stopping. These values agreed well with the design values used.

After the first glide flight and landing, the air pressure was increased in the main gear air-oil strut and a new metering pin installed to increase the energy absorption capacity. This did not prevent the main gear strut from very nearly bottoming on subsequent landings. A second revision was made in which the total strut travel was increased approximately ten per cent and this, plus a further increase in the strut air pressure, has proved to be satisfactory.

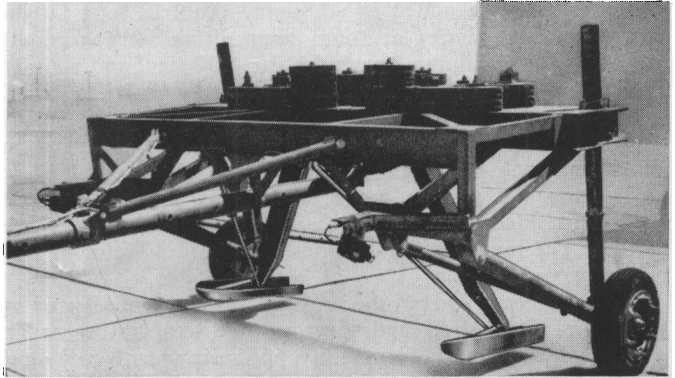


Figure 30. Landing gear test trailer.

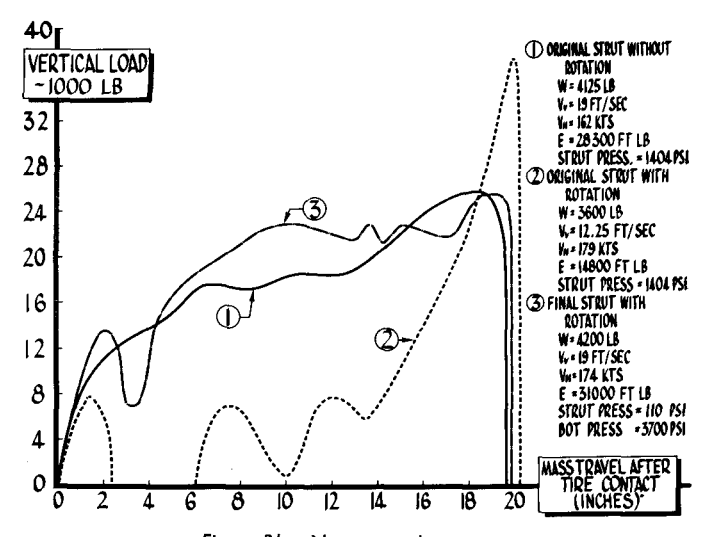


Figure 31. Nose gear drop tests.

During early landings of the X-15 it was found that the nose wheel tyre marks left on the dry lake bed were not continuous. After initial contact the tyre marks became very faint or disappeared for short distances, then became distinct again. This puzzled the engineers responsible for the design of the gear and an investigation was made into the cause for this erratic behaviour. All preliminary drop tests of the gear had been satisfactory and preflight servicing of the gear had been checked. This was important because a shrink strut contracted the shock strut to the fully compressed position during stowage in the aircraft. After retraction of the gear prior to launch, dry nitrogen gas was pumped into the strut at a final pressure of 1404 psi. Upon lowering the gear to the extended position, the nitrogen gas was trapped below the orifice while most of the oil was trapped above. The design of the metering pin was such as to prevent a rapid change in position of the oil and nitrogen during the time from gear extension to wheel touch-down. The elapsed time for this action was ten seconds. The result was that the normal functioning of the strut was only partial and thus had low efficiency. To check this phenomenon, new dynamic tests were made with the originally configured gear dropped as in the preliminary tests made during the design period. The gear was installed on the drop rig in the extended position and serviced as required. A plot of the vertical wheel load against the mass travel for this configuration, as well as pertinent parameters, is shown in Fig. 31, curve (1). The performance appears perfectly normal for an air-oil shock strut-wheel-tyre combination found on any contemporary landing gear. The drop test rig was then altered to permit the gear to be installed in the retracted position. Tests were then started at a low energy level. The wheel was first spun to equivalent landing speed, then released from its stowed position, and after a time lapse of ten seconds dropped as before. This procedure quite accurately reproduced the gear behaviour during an actual landing. The result is shown in curve (2) of Fig. 31. It will be noted that at a relatively low energy level (14 800 footpounds), a skip occurred since the vertical load reduced to zero after initial contact. Likewise, the maximum vertical load at the end of the stroke reached 37 000 pounds which exceeded the maximum design value at this point of 30 000 pounds. Since the required energy level was approximately 30 000 footpounds, it was obvious that an improvement in strut performance was mandatory.

The first approach was a modification in the shape of the metering pin, but this failed to achieve the desired results. After some additional exploratory drops, it was decided that

all high pressure air had to remain out of the strut until it was rotated to the landing position and the oil contained below the orifice. This would prevent aeration of the oil which had occurred before. Tests were halted until a small bottle of high pressure air (nitrogen) was installed on the strut. The air could be bled into the strut by means of a valve actuated as the strut reached the extended position. The air capsule was sufficiently compact to permit its installation on the strut and for maximum reliability was installed in duplicate. The stored air was at a pressure of 3700 psi. This system worked satisfactorily and the load-stroke curve (3) for this configuration is shown in Fig. 31. A later change replaced the air bottle with the floating piston separating the air and oil inside the strut.

WINDSHIELD DESIGN

The windshield design and analysis was interesting from several points of view. The windshield is composed of a single outer pane and a double inner pane (Fig. 32). The maximum air pressure on the outer pane is 7.8 psi gauge, above 35 000 feet and 9.3 psi gauge below that altitude, while the cabin pressure is maintained at 3.5 psi gauge. The outer panel is alumino-silicate plate glass with a temper of 25 000 psi and is $\frac{3}{8}$ inches thick. The inner panel is laminated with two panes of soda-lime plate glass and a silicone type "K" interlayer and tempered to 14 500 psi. The analysis was complicated by the fact that not only were the design parameters and strength rapidly changing with time, but the windshield frame was tri-metal. The basic retaining frame was Inconel with a titanium (6Al-4V) outer glass retaining strip and aluminium alloy inner flange elements. The outer surface of the glass was designed to reach a temperature of 800°F while the inner surface of the outer glass was to reach a temperature of 550°F. The inner surface temperature, however, lagged behind the outer surface temperature. During the rapid heat up, a maximum temperature differential of 480°F occurs at a time when the outer surface temperature is only 570°F. The mutual restraint of the glass panels and supporting frame further complicated the final stress distributions. The maximum panel stress in the outer glass occurred at the edge with a magnitude of 8750 psi. The maximum combined pressure and thermal stress, however, occurred in the centre of the panel with a magnitude only slightly higher or 9150 psi

The strength of the outer glass is dependent on time at elevated temperature. From data supplied by the glass manufacturers, the strength of the glass was calculated to be 17 110 psi after 10 hours at load and sand blasted. The latter surface condition was assumed since it was conceivable that some surface damage might result after continued

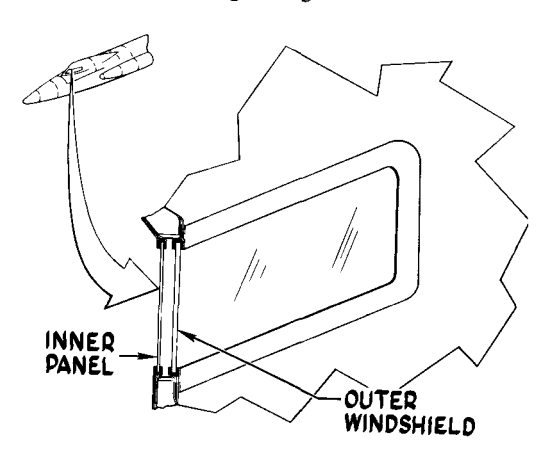


Figure 32. Windshield configuration.

service. The glass panels, before approval, were each subjected to a pressure test of 55 psi gauge for one hour on each side at room temperature. The size of the panels is 8.4×28 inches and for the test they are supported along the edges. Each panel is further subjected to a thermal shock test by first heating to 550° F in a salt bath for 3 minutes and then plunging the panel in a bath of tap water at room temperature.

The changes from the original design consisted of a change from sodalime to alumino-silicate glass in the outer panel and a change from the Inconel X outer retaining strip to titanium alloy. These changes were brought about as a result of flight tests involving high values of heating. The alumino-silicate glass was introduced because of higher strength at temperature, improved heat conductance and a lower thermal coefficient of expansion. The titanium alloy retainer had a lower thermal coefficient of expansion.

PRESSURE VESSELS AND TESTS

The table shown in Fig. 33 lists the principal pressure vessels used to store the helium and hydrogen peroxide propellant. The vessels ranged in size from 6-32 inches in diameter for the spherical shapes, a 14 inch diameter \times 96 inches long cylinder and a prolate spheroid, $15\times28\cdot5$ inches. Temperatures varied from $-300^{\circ}\mathrm{F}$ for the cryogenic oxidiser to $+160^{\circ}\mathrm{F}$ ambient in the engine compartment.

In the design of the vessels, considerable importance was placed on the relation of working pressure to the yield strength of the materials used. In the table is listed the normal working pressure for each vessel. Helium gas was stored at a pressure of 3600 psi while the expulsion pressure for the $\rm H_2O_2$ was 600 psi. Since relief valves require tolerance in their setting, over-pressures may result. Consequently, the maximum relief valve pressure limit was also considered.

The third consideration was the design proof pressure, which generally was selected to be 50 per cent greater than the normal working pressure. Proof pressure stress levels were selected so as not to exceed the tensile yield strength of the material. This relationship is shown in the columns listing calculated stress data. In general, the stresses at proof pressures were less than the yield stress, except the aluminium alloy prolate spheroid. In the latter, equality was permitted but the proof pressure was more conservatively selected at 175 per cent of the working pressure. The same ratio was used in the design of the 32 inch diameter sphere also containing H₂O₂. Working pressure stress levels varied from 45·1-61·3 per cent of the yield stress. A 50 per cent level was sought for this presssure level and, as will be noted, was generally achieved. Before being considered acceptable, a full scale specimen of each vessel was subjected to cyclic pressures using the relief valve setting as a criterion. Because of the limited life of the air vehicle, a test of 2000 cycles was estimated to be adequate. This was achieved without failure at the extremely cold temperatures and with high cycles at room temperature added as additional proof of long fatigue life. The high cycles at room temperature were generally held to 8000 maximum except for the 4130 steel and 6061-T6 aluminium alloy vessels where they were increased to 10 000 cycles. There was no failure in the 32 inch diameter sphere after 3380 cycles at which time the specimen was reserved for other tests. A specimen of each vessel was pressurised to destruction. It will be noted that failing pressures yielded factors of safety greater than 2.0 for eight of the nine types tested. The remaining tank so tested yielded a factor of 1.92 which was acceptable.

The materials used in the pressure vessels were selected on the bases of yield strength over a wide temperature range, toughness, weldability, formability, and resistance to corrosion. Their general characteristics are shown in Fig. 6. The

Size and shape	Contents	Service temper- ature	Materials	Pressures (p.s.i.)			Calculated stress		Test results			
				Work- ing	Max. relief valve setting (PRV)	Design proof	Work- ing stress %F _{ty}	Proof stress %Fty	P _{RV} cycles at room temp.	P _{RV} cycles at low temp.	Burst pressure (p.s.i.)	P BURST
16 in. dia. sphere	He	+160 -100	6AL-4V Ti	3600	3900	5400	49.5	74 · 2	8000	2000	9340	2.59
32 in. dia. sphere	H ₂ O ₂	+120 + 35	350 Cres (175 k.s.i.)	600	650	1050	53.7	95.8	3380		1150	1.92
14 in. dia. cyl. 96 in. long hemisph. ends	He	+120 -300	Inconel X 6AL-4V Ti	3600	3900	5400	61·3 50·2	92 75·4	8000	2000 (-300°F) 2000	8650 8975	2·4
23·75 in. dia. sphere	He	+120 -300	Inconel X 6AL-4V Ti	3600	3900	5400	59·5 49·5	89·3 74·2	8000	2000 (-300°F) 2000	8000 8890	2·22
6 in. dia. sphere	H _e	+160 - 65	4130 s.t.l. (130 k.s.i.)	3600	3900	5400	49 · 1	73.6	10000		8800	2 · 44
12 in. dia. sphere	He	+160 - 65	4130 s.t.l. (160 k.s.i.)	3600	3900	5400	45 · 1	67 · 7	10000	_	9400	2.61
15·5 in.×28·5 in. prolate spheroid	H ₂ O ₂	+120 + 20	6061-T6 Alum.Al.	600	700	1050	54·3	100	10000		1600	2.67

Figure 33. Pressure vessels.

materials originally selected for use at the cryogenic temperatures were Inconel X, two titanium alloys, 6Al-4V and 5Al-2.5Sn, and 350 CRES. Before proceeding too far with the design, however, a series of low temperature impact tests was conducted. The specimens were an 8 inch diameter sphere using 5Al-2.5Sn titanium alloy and two cylindrical specimens with hemispherical ends (8 inch diameter $\times 14.5$ inches long) made from Inconel X and 350 CRES. All specimens were designed for welded construction. Each specimen was first subjected to a minimum of 2000 cycles of internal pressure equal to 80 per cent of the calculated burst pressure. The specimens were again pressurised to the 80 per cent value and subjected to impacts supplied by a hammer impinging on a striker pin one inch in diameter with a rounded point having a $\frac{3}{16}$ inch radius. The tests were run at room temperature and at -300-320°F. In each case, the striker pin was aimed at the circumferential weld area. Impact began at 5 foot pounds and gradually increased until failure occurred or the test stopped. The results proved interesting.

The impact tests at room temperature involved only the Inconel X and 350 materials. The Inconel X tank suffered a puncture type failure after a second impact at 90 foot pounds. The 350 tank after 18 progressively increasing impacts failed by a puncture at 92.5 foot pounds aimed at a point of previous impact. The test results at $-300-320^{\circ}F$ were quite different. The 350 specimen failed at the first impact of 5 foot pounds and the resulting failure was explosive in nature. The Inconel X specimen tested at $-310^{\circ}F$ failed via a puncture type failure after six impacts of 60 foot pounds each. The titanium specimen on the other hand, when tested at $-320^{\circ}F$, did not fail after 5 impacts of 62.3 foot pounds, even though each of the five impacts was aimed at the same place. Thus, Inconel X and titanium were selected for use in pressure vessels where extremely low temperatures were involved.

The titanium alloy used in the impact test specimens was 5Al-2·5Sn. A later alloy, 6Al-4V, having similar characteristics to the 5Al-2·5Sn but higher yield strength, was used throughout the design of pressure vessels. The principal reason for this change was the excessive grain growth in the weld heat affected zone of the 5Al-2·5Sn alloy.

The largest of the spherical pressure vessels to be built was 32 inches in diameter and operates at 600 psi in a normal temperature environment of +35 to $+120^{\circ}F$. The materials used were 350 CRES steel for the shell and 355 CRES fittings. The heliarc welding process was used. The tank was heattreated after welding using a low internal pressure of argon. The presence of the argon prevented formation of scale and preserved the tank contour. Test tanks were pressurised to destruction with volume changes measured during the tests. It was found that tanks aged at 950°F absorbed approximately four times the energy absorbed by a tank aged at 850°F, at the same time exhibiting very little difference in yield and burst pressures.

The two small spherical tanks made from 4130 steel were patterned after existing designs readily available and well proved for use in the temperature range indicated.

The prolate spheroid, because of severe forming problems, was made from 6061-T6 weldable aluminium alloy. To prevent catalysis of the H_2O_2 decomposition, a bladder type liner was required and this was especially developed for this purpose at North American Aviation, Inc. It is a special elastomer comprised of a mixture of Viton and silicone rubber. The liner has performed satisfactorily under all conditions.

The discussion of the pressure vessels used in the X-15 would not be complete without mention of some of the qualification tests conducted to assure airworthiness. In addition to the proof, cyclic and burst pressure tests previously mentioned other tests were conducted. The most severe series

of tests were vibration tests at resonant frequencies about each of the three principal axes. These tests consisted of vibrating at +5 to +10 g's from 10 cps to resonant frequency back to 10 cps gradually varied during a 15 minute cycle. The duration of each test was 1.5 hours. Slosh tests were performed with the vessels partially full of fluid under pressure and subjected to 1g acceleration in both a longitudinal and transverse direction for as many as 5000 cycles. Fluid resistance tests consisted of cyclic heating the tanks containing 90 per cent pure H_2O_2 to moderate temperatures for prolonged periods. There were also combined slosh, vibration, and expulsion tests conducted on the aluminium alloy tank and high acceleration tests were run on the 32 inch diameter H₂O₂ tank. The latter was pressurised when tested on a catapult test rig. So far, all tanks serving as pressure vessels on the X-15 have performed satisfactorily.

Structural Testing

Many structural tests were conducted during the design of the X-15, including both structural elements as well as representative sections of the principal components. In view of the fact that nearly all of the high temperature surfaces were made of unreinforced sheets of comparatively new materials, considerable testing of plain sheet elements was performed. The influence of high temperatures and thermal gradients also influenced the decision to test liberally. There were, however, no tests made of actual air vehicle components. In retrospect, the testing, which was done during design, yielded gratifying results and, on the whole, verified the approaches taken.

WING BOX

One of the first component simulation tests was performed on a box beam representative of the wing structure. Fig. 34 shows a full-scale test box which was subjected to ultimate loads and transient heating conditions equal to those of the X-15 wing. The box is shown with the upper cover removed. The box beam, which was 48 in \times 26 in \times 6.5 in, was made from Inconel X skins and titanium-alloy spars. The two intermediate spars have corrugated webs attached to scalloped cap angles (two angles on compression surface and one on tension surface). The attachment for the skin to the spar caps consisted of $\frac{3}{16}$ in diameter Inconel X flush screws which were spaced one inch on centre. No chordwise reinforcements were incorporated. The purposes of the tests were as follows:

(1) To determine the effects of transient heating, thermal

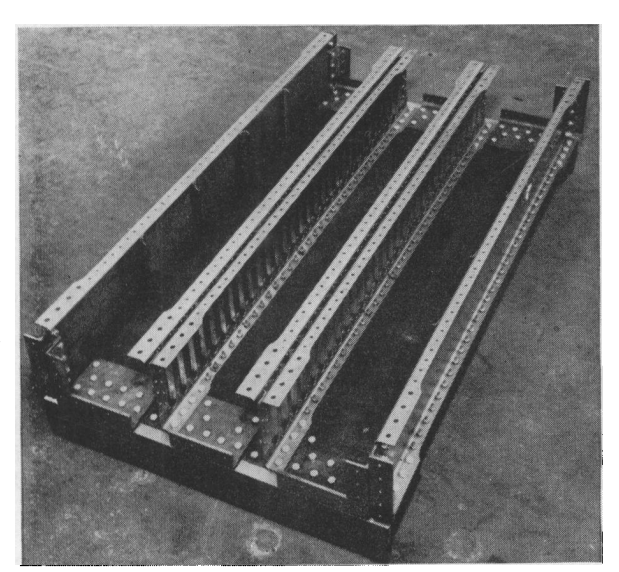


Figure 34. Wing test box.

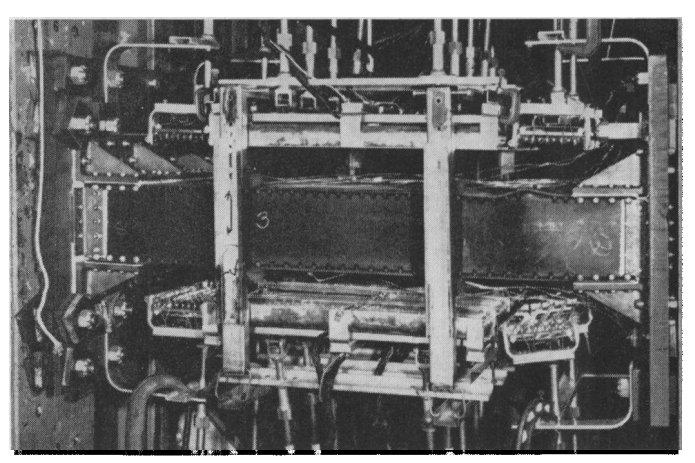


Figure 35. Wing box test.

gradients, and bi-axial thermal stresses on the buckling and ultimate strength of a box beam.

- (2) To determine the magnitude of thermal deformations for varying load levels, temperatures, and gradients.
- (3) To determine the influence of thermal stresses on structural attachments.
- (4) To ascertain possible creep effects due to repeated loads and heating.
- (5) To evaluate importance of steep thermal gradients on flat web spars in the presence of bending stresses.

Figure 35 shows the instrumentation and set-up for the wing box test. The box was attached to a rigid jig at one end and a floating jig which was designed for pure bending application was attached at the other end. General Electric T-3 lamps were used as heating elements. Precautions were taken to delete any extraneous influences for the case of thermal loading. This was accomplished by elongating the jig attachment holes in the chordwise direction. Asbestos pads were employed between the box skins and the jig plates to reduce heat losses. Additional heat was concentrated at the ends of the box to minimise gradient differences between adjacent skin elements and to prevent premature buckling and unrealistic thermal stresses in the skin covers. Thermocouples were installed on the inside and outside surfaces of the cover plates and were also added on the flanges and webs of the spars. Temperature readings were recorded during each test.

The wing box was subjected to a series of tests designed to demonstrate its strength, thermal effects, and combinations of both. The tests were as follows:

- (1) The box was first subjected to heat alone. This was done by simply supporting the four corners and heating the upper surface to 830°F and the lower surface to 990°F. The heating period was 100 seconds. No buckles appeared in the surfaces.
- (2) Next, the design ultimate bending moment was applied at room temperature. Sizeable compression buckles existed under this condition. Upon removal of the load, all buckles disappeared.
- (3) With the upper and lower surfaces heated as in the first test, a moment equivalent to 85 per cent limit was applied. Under this combination the skin buckles had a depth of $\frac{3}{16}$ in. At limit load, the buckle depth remained approximately the same.
- (4) The aforementioned sequence was followed by a variety of load and temperature combinations during which the upper surface reached 450°F and the lower 810°F. This represented the maximum temperature differential. Inspection

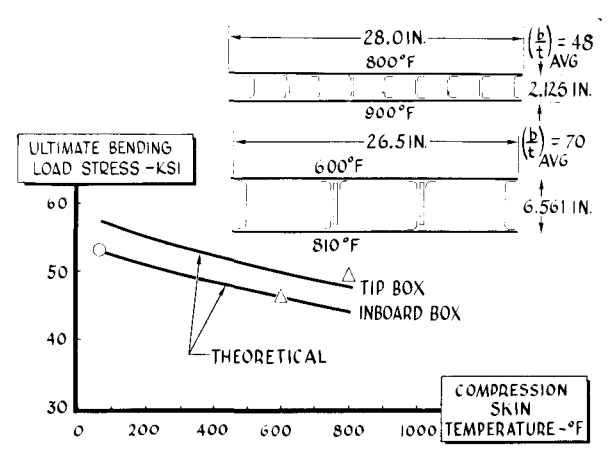


Figure 36. Multi-spar test box.

of the box after the completion of all limit load and temperature tests revealed the fact that all buckles had disappeared.

(5) Finally, with the upper surface at 600°F and the lower at 810°F, the box failed at a moment equal to 116 per cent of the calculated strength. The failure ran slightly diagonally across the box, approximately 6 in from the loading jig. After removal of the load and cooling to room temperature, the unfailed portion of the box had no permanent buckles.

In addition to the wing box test described, a second box representing the outer portion of the wing was constructed and tested. The tip box was tested similarly to the inboard box with appropriate temperatures. The results for both boxes are plotted in Fig. 36. The graph shows ultimate strength plotted against compression surface temperatures. The failure of the tip box is shown by the triangle at 800°F. It is compared with the theoretical curve which is calculated for no thermal stress. The agreement is excellent even though elastic theory would have predicted a thermal stress in the cover amounting to approximately 40 per cent of the direct bending stress at 800°F. The box failed in wide flange buckling across the entire surface but did not collapse. The load carried after failure was nearly the same as at the time of failure. At limit load and temperature gradient the box had some buckling which did not remain permanent.

The inboard box did fail in local buckling and is shown by the triangle on the lower curve. As in the former case, the theoretical thermal stress was 15 per cent of the direct bending stress but agreement with simple theory showed negligible thermal stress effects. For added information, the circled point represents the failure at room temperature of an earlier box beam which also shows good agreement with theory.

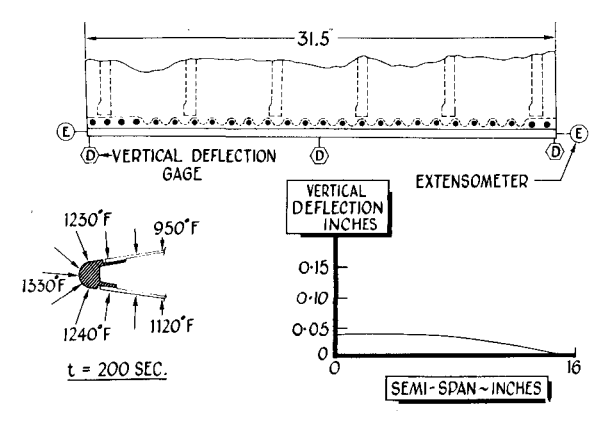


Figure 37. Leading edge nose piece test.

STAGNATION POINT TEST

At the top of Fig. 37 is a sketch representing one of the segments of the wing leading edge. The ribs are titanium and A-286 fasteners were used for attachment. The Inconel X heat-sink mass is shown by the hatched area.

The purpose of this test was to investigate the behaviour of the leading-edge structure and attachments when subjected to high temperature gradients caused by the local stagnation point "hotspot." The stagnation-point mass was heated to 1330°, giving a chordwise gradient of 830° per inch at the nose. After the test the only damage to the specimen was a permanent set in the end fastener holes equal to $1\frac{1}{2}$ per cent of their diameter. This was well within the acceptable permanent-set range for fasteners. The maximum spanwise bow in the specimen during the test was 0.03 in. The specimen was cycled five times to the design temperature. No additional permanent set occurred in the holes and no other damage appeared.

After this test, an exploratory series of tests was run at increasing temperatures to determine the strength of the specimen under high thermal gradient. There was no additional damage to the specimen under the maximum temperatures producable by the laboratory heating equipment. The maximum temperature distribution attained during these tests was 2100° at the nose, 1800° on the skin, and 1300° in the titanium nose rib. These temperatures exceed the generally accepted usable range of these materials. However, in this configuration, which is loaded almost entirely by thermal expansion, no damage was visible. This means that in actual flight, the leading edge would not suffer from at least one exposure to these temperatures.

WING LEADING EDGE

Another test was conducted on one of the leading-edge skin panels to determine whether, under design load and temperature, there would be any aerodynamically significant deformations. The leading edge was loaded to its design loading and was heated to 1100°. Deflection measurements were taken at the centre of one panel and at the nose. The test results are shown in Fig. 38. In the upper graph, the vertical deflection of the panel centre-line relative to the front spar and nosepiece is plotted against length. In the lower graph, the deflection of the panel centre relative to its supporting ribs is plotted against width. The panel developed a single-wave deformation under either heat or load alone, with a maximum deflection less than in the combined case shown here. A maximum deflection of the nose relative to the front spar of 0.37 inch occurred during the test. These deflections were not considerd to be serious.

WING-FUSELAGE "A" FRAME TEST

A test was also made to verify the strength of the wing-tofuselage transition structure, or "A-frame structure".

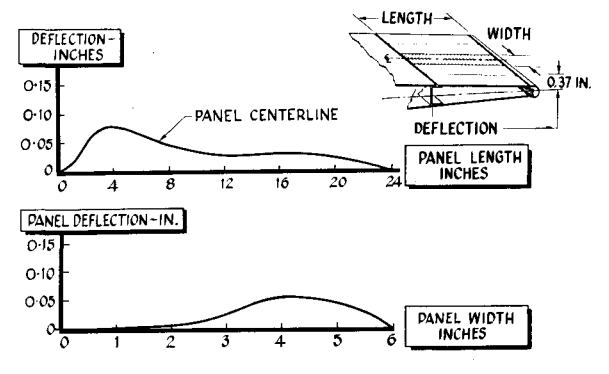


Figure 38. Test for panel deflection, heat and load.

Figure 39. Wing A-Frame thermal test.

This specimen incorporates, as fore and aft boundaries, two of the fuselage-tie A-frames, an intermediate A-frame, a portion of the root rib, and enough of the inboard wing box to distribute the test loads properly. The specimen was loaded to ultimate design loads and temperatures. The temperature on the lower A-frame surface was 1125° and the temperature on the adjacent lower wing surface was 975°. There was no residual permanent set after the test, even though buckles appeared in the A-frame intermediate panels on the application of temperature. The chordwise distribution of bending stress at section A of the wing box was measured by strain gauges at room temperature and is shown in Fig. 39. The effect of the unsupported intermediate A-frame is quite apparent and the test results agreed with analysis.

FRONT SPAR TEST

The front spar is subjected to high temperature gradients through its depth and, consequently, high thermal loads are generated in the web and in the attaching fasteners to the spar-caps. To investigate this condition, a full-scale front spar specimen was cycle-tested under design temperature gradients. The sketch in Fig. 40 shows the spar and the flange temperatures. The temperatures were cycled 50 times from room temperature to the maximum values. The thermal stresses in the centre of the web and the permanent deformations of the spar web and end-fastener holes were recorded during the cycling. Results of the test are shown in the figure. The curve shows theoretical deflection and the four circles are test points. After the tests were completed, there was a permanent vertical tip deflection of 0.20 in relative to the root. The spar had also crept spanwise 0.1 per cent.

A strain corresponding to a thermal tensile stress of 65 000 psi was indicated by a strain gauge at the centre of the web during the last cycle. This stress level had decreased during the cycling. Later the cycle tests were repeated on a spar with web lightening holes, such as now exist in the aeroplane inboard spar. The indicated web stress was reduced by 30 per cent. The four end spar fastener holes were checked for permanent set periodically during the tests. The permanent set increased fairly rapidly at first and then levelled off, approaching a constant value at the end of the cycling. The maximum permanent set occurred in the inboard holes and amounted to approximately 10 per cent of the hole diameter. Theoretically, on an elastic basis, the level of thermal stress measured in the web should have failed the spar fasteners, but apparently the combination of plastic relief and friction relieved the fastener loads enough to avoid any shear failure.

HORIZONTAL TAIL BOX TESTS

Tests were conducted on a series of box structures representing the horizontal tail. The chief purpose was to satisfy the torsional stiffness requirements for flutter. Test

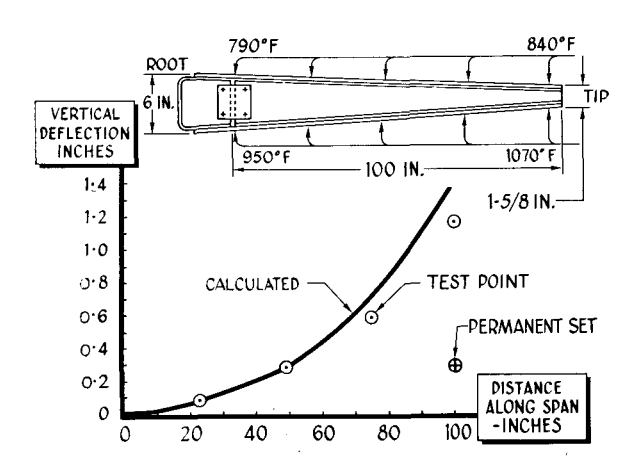


Figure 40. Front spar thermal deflection test.

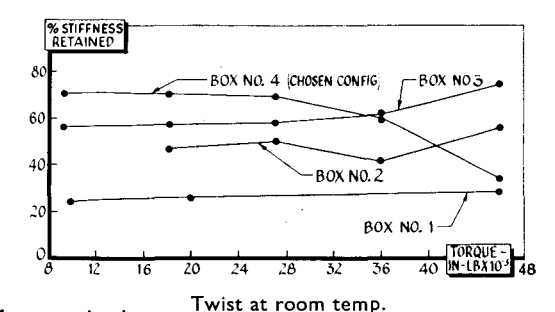
boxes were constructed with varying rib spacing, material, rib web thickness, and outer skin gauge. The governing test parameter was the torsional stiffness remaining after thermal skin buckling and application of high torque loads. The tests were conducted by applying the torque in increments up to 45 000 inch-pounds and applying heat after each increment of loading. The data are plotted as the ratio of twist at elevated temperature to twist at room temperature against torque at the various levels. They thus indicate the percentage of torsional stiffness retained.

Four boxes were tested and are numbered in chronological order of testing. Box 3 gave satisfactory stiffness but had thick skins. Consequently, a lighter configuration was sought. Box 4 had lighter skins and the improved stiffness over boxes 1 and 2 was attained by modifying rib spacing, material, and design. Box 4 had satisfactory stiffness and was chosen as the configuration for the aeroplane.

The curves of Fig. 41 do not show the comparison of actual stiffness in the boxes, but the ratio of stiffness hot to stiffness cold. Box 4 was actually stiffer than box 2 over the whole torque range. However, subsequent changes in external temperatures and loads made necessary a redesign to heavier skin gauges and modified rib material. There was no further testing since the revised configuration exceeded the stiffness requirements. A bending test, under design temperatures, was performed on one of the boxes with a leading edge attached. The slotted leading edge relieved the thermal stresses as expected and the box failed at a stress in good agreement with calculations. All loadings used in this series were in excess of the design limit.

FUSELAGE SPECIMEN

During the design of the fuselage, a full scale test specimen was constructed and a series of tests was undertaken which



%Stiffness retained = Twist under thermal gradient

Figure 41. Horizontal tail box test.

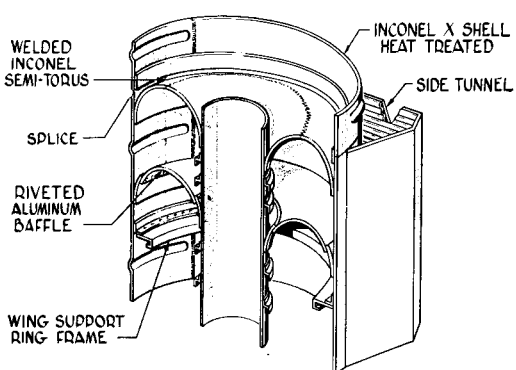


Figure 42. X-15 fuselage test specimen.

included internal pressurisation, external loads, and temperature environment. The test component was a generalised section of the fuselage in the region of the integral propellant tanks. It was basically a 56 in diameter cylindrical shell 80 in long with a $14\frac{1}{2}$ in diameter inner cylinder, two toroidal bulkhead frames, and two side fairings. The details are shown in Fig. 42. The outer shell was 0.093 in Inconel X sheet across the top and bottom and 0.040 in the beaded side skins. Welding was used for assembly except for a mechanical joint at Station 60. Beads were formed in the side areas to provide thermal relief in the longitudinal direction. One typical wing carry-through frame was welded to the shell at Station 16 with four attaching fittings for external loads. Four longitudinal angles were welded to the outside of the shell to serve as fairing attachments. The $14\frac{1}{2}$ in inner cylinder was fabricated from 0.043 in Inconel X material and Z-section circumferential stiffeners were spotwelded to the outside. One of the toroidal bulkheads consisted of two circular segments made from Inconel sheet welded to the large shell wall and the inner cylinder respectively. To these were riveted a 0.050 in thick 7075-T6 clad aluminium alloy section to complete the torus. The other torus was formed in two segments welded to the outer and inner cylinders and along a circumferential seam joining the two segments. Only one fairing duplicated the design which consisted of a flat outer sheet reinforced by a corrugated inner sheet—both made from Inconel X.

The first test was an internal pressure test to determine the collapsing strength of the aluminium alloy torus (Fig. 43(a)). Pressure was applied above the aluminium torus and failure occurred at 10.7 psi which was 71.3 per cent of

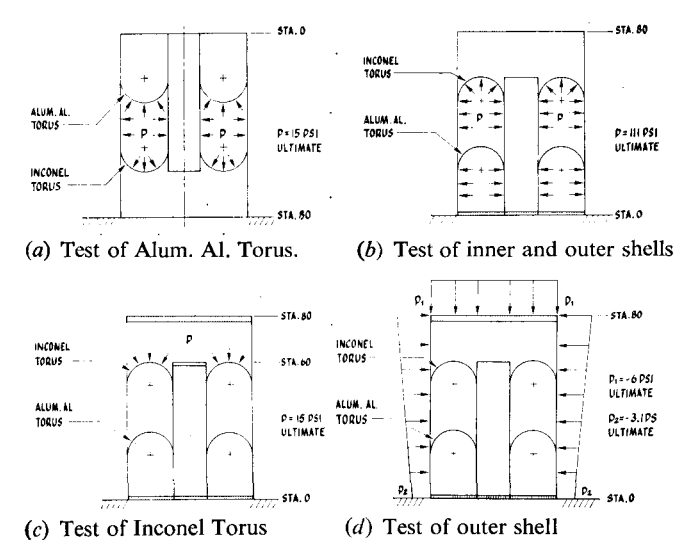


Figure 43. Test of fuselage specimen.

the required pressure. A series of baffle specimens was made using various sheet thicknesses and stiffeners. It was concluded from these tests that radial stiffeners spaced 15 degrees apart were required to sustain the 15 psi pressure.

The object of the second test was to test the welded joints of the Inconel torus, the welded joints of the outer shell, and the strength of the inner shell under a collapsing pressure (Fig. 43(b)). Positive pressure was applied internally between Station 0 and the Inconel torus. Failure occurred by compression buckling of the inner shell at 80 psi and was in a multi-node fashion as indicated by theory. As a result of this test, the inner cylinder stiffener spacing was reduced in order to carry the required ultimate pressure of 111 psi. Both the Inconel torus and main outer shell withstood the pressure without failure. In addition, 100 cycles of limit pressure (74 psi) were also applied without damage.

The third pressure test was to test the Inconel torus for compression loads caused by negative pressure in the centre propellant cell. For this test, the specimen was closed with a steel bulkhead at Station 80 and a cap placed on the centre cylinder. Hydrostatic pressure was introduced in the space shown in Fig. 43(c). The test was successfully completed to 20 psi ultimate without failure.

Following these tests, a negative pressure test of the outer shell was conducted (Fig. 43(d)). For this test, a sealed bulk-head remained attached at Station 80. To prevent premature failure, the specimen was filled almost full with de-ionised water. The space at the top was evacuated to -6 psi with no failure resulting. Due to the head of water within the specimen, the net pressure at the bottom was -3.1 psi. This test was sufficient to demonstrate the collapsing strength of the outer shell.

The next order of tests included both room and elevated temperature load tests of the wing carry-through frame. The specimen was loaded through a set of loading beams attached to the wing fittings (Fig. 44). During the room temperature test, the frame failed at 93 per cent design ultimate load. Since failure occurred only on one side, a repair was made and the frame retested to a temperature gradient across the frame of 555°F. The gradient was obtained by first cooling the inner flange of the frame with a fine spray of liquid nitrogen. Quartz glass radiant heaters were used on the outside. The temperature gradient was programmed to achieve a maximum value in 300 seconds. Limit load was first applied at room temperature and, while holding the load constant, the temperature gradient was achieved. Next the load was increased and failure took place at 90 per cent design ultimate load. The failure was at the same corresponding location on the side of the frame opposite to the previous failure. A reinforced frame was used in the final design. It is interesting that there was only a 3 per cent difference between the identical failures at both room temperature and with the gradient noted above.

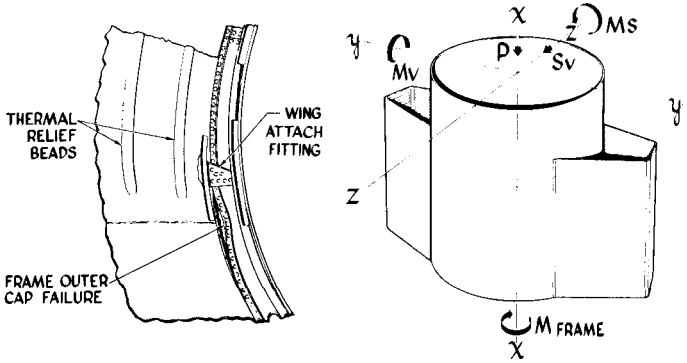


Figure 44. Frame failure test.

Figure 45. Fuselage specimen tests.

Figure 46. Fuselage skin temperature plotted against time

The specimen was then loaded in vertical bending (M_{y}) Fig. 45) both at room and elevated temperatures. Moment was applied through a steel bulkhead and loading beams attached to Station 80. It was necessary to pre-cool all four side fairing attach angles to $-200^{\circ}F$ before heating to achieve the proper temperature gradient. The room temperature load tests were carried to the required ultimate moment of 6 300 000 inch pounds without failure. The elevated temperature tests, to a gradient of 550°F, were run at increasing load levels (10 per cent increments) with a cool-down after each load level. In every case the cool-down was followed by load application and then the heat reapplied. Failure of the outer shell occurred at 110 per cent design ultimate load as the heating cycle was applied. Fig. 46 shows a plot of significant surface temperatures against time for both the vertical and side (horizontal) bending cases and Fig. 47 shows the fuselage specimen after test.

The remaining bending test was a side bending case in which the side fairing was placed in compression. (M_{\circ} Fig. 45). This test, like the preceding one, was conducted both at room and elevated temperatures. The test set-up was also the same as for the vertical bending. In addition to the side bending moment of 2 940 000 inch pounds, an axial compression of 9900 lb was applied to the side fairing. At room temperature, the main shell withstood 100 per cent side bending moment, but the side fairing failed at 43 per cent maximum load through the spotwelds connecting the outer skin to the corrugated inner skin. The spotwelds were replaced with monel rivets and the fairing failed at 85 per cent at a section which was beyond the support of the inner corrugated skin and hence of no real significance. The spotwelding used in the specimen was changed to a stitch weld of greater strength in the vehicle side fairing, to achieve 100 per cent strength. During the elevated temperature part of the test, the outer shell withstood 150 per cent design ultimate bending moment without failure but during a subsequent loading the outer shell failed at 140 per cent design ultimate load.

The final major test was a transverse shear test in which an

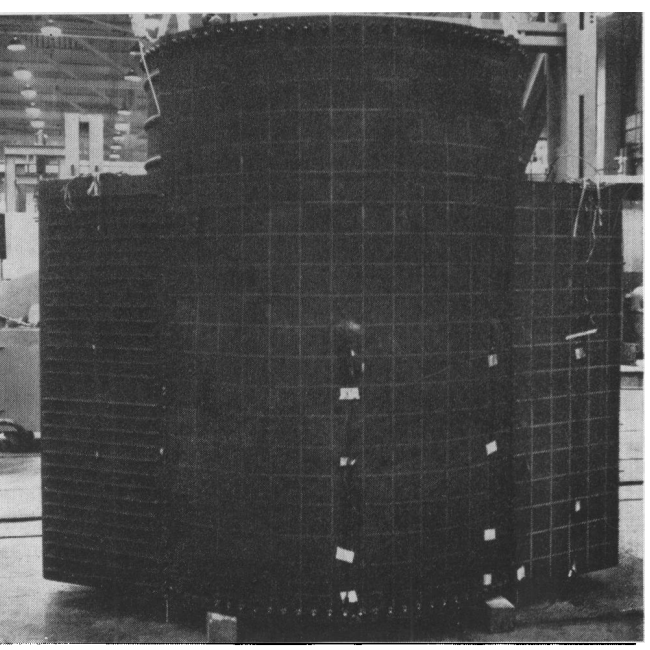


Figure 47. Fuselage specimen after test.

ultimate load of 46 700 lb was applied at Station 80 and reacted at the floor mounting. This test was conducted at room temperature and was completed without failure.

This series of tests on a major fuselage specimen proved to be highly successful both from a design and test technique standpoint. Sufficient data were acquired to complete the design with confidence, while considerable advancement in static testing technique resulted from this exercise.

Conclusions

The structural design of the X-15 was completed in a timely manner considering the resources available. As noted in the introduction, most of the research in materials and structural science had been completed when the design was undertaken. There remained, however, much work to be done in the field of human life sciences—including escape, the use of materials at extreme temperatures, and the establishment of high reliability in all flight sustaining systems. To some extent all of these affected the structural design in some way. Of equal importance, perhaps, was the development of fabrication and assembly techniques even though methods for doing so did exist. Nevertheless, the challenge of each problem was met with a practical solution whereas more clearly optimum solutions would now be possible. It is doubtful that with current knowledge, any basic changes in the selection of structural materials or configuration would result. Of this we can be certain: the X-15 has added much to the knowledge of flight within and outside the earth's atmosphere and has raised man's confidence in projecting space flight.

Discussion

E. Loveless (English Electric Aviation, Assoc. Fellow): Dr. Schleicher had given them a very comprehensive review of a most interesting aircraft. He had had the privilege of reading the paper which, as Dr. Schleicher indicated, had had to be cut short and it gave even further detail. From this one gathered the amount of design work which went into the aeroplane, but what was more important he thought, was the

practical experience of building the aircraft and the amount of flight data which had been obtained. It was experience and data which they had not got in this country, unfortunately. All of them, he thought, would like to ask many questions and he would like to deal with a few points.

Figure 15 in the paper showed the attachment of the wing root by the nine "A" frames and then the five fuselage frames.

Fig. 16 showed the variation in temperature chordwise along the wing. Dr. Schleicher also mentioned, of course, the low temperature from the LOX. Therefore, there was inevitably a large change in temperature between the wing and the fuselage going chordwise in this area. Would Dr. Schleicher tell them whether these temperature variations were taken entirely by thermal stresses in the structure of the wing and fuselage, or did they allow joints on the "A" frames to the fuselage frames to slide at all fore and aft, locating only one in a fore and aft direction? This was a point of great interest, because if it were done in this way, he would like to know if the sliding action worked satisfactorily under the wing loads.

Another point was this question of addition of thermal stresses and load stresses. Quite obviously, up to the yield point the addition of strains and the addition of stresses was the same thing, but once one had passed the yield point one could add a thermal strain to a load strain without increasing the resultant stress very much and was this not what happened? Dr. Schleicher indicated this in a number of cases, although, to his disappointment he said he had added the thermal stress to factored loading stress, he thought, in arriving at an ultimate. This was a source of considerable argument and discussion between Airworthiness Authorities at present.

One point mentioned in the paper was the problem of acoustic fatigue on the X-15 in the noise field of the jets of the B-52 and the fact that certain detailed changes were made in the structure because of this. Had they no noise problem when the X-15 was in free flight either from the noise of its motor or from the boundary layer noise, and consequent panel buffeting? Had they covered this acoustic problem by ad hoc testing of various types of structure or had North American had design data sheets for those which they felt could then cover the structure for acoustic problems?

He thought Dr. Schleicher had mentioned that a liberal amount of testing was carried out on specimens but none on the actual air vehicle components. Had they measured loads in flight at all, either by measurement of pressure, or could they in any way measure strains in flight? Did the rapidity of temperature variation render strain gauging impossible?

Dr. Schleicher: Concerning the temperature variations at the root of the wing, the design of the "A" frame attachments was such that fore and aft movement due to thermal expansion was possible at all frames. The centre frame had less clearance than the others. The wing drag forces were taken through the skin of the side fairing. This arrangement had worked satisfactorily despite the small relative movement encountered.

Thermal stresses were computed for both spanwise and chordwise temperature distributions and added to load stresses up to limit load values in practically all cases. In general, they were not added to the design load stresses (limit loads × factor of safety). Mr. Loveless was quite right that thermal strains beyond the elastic limit did not indicate large stress changes. The magnitudes depended on the stress-strain curve for the particular material under consideration.

The acoustic problem was resolved by ad hoc testing of panels in the sound chamber. One main concern was the sound excitation from the two inboard jet engines of the B-52. The noise levels reached a peak value of 156 decibels over the tip of the horizontal tail. Chamber tests up to discrete noise levels of 158 decibels had been made on representative structures. The structural changes referred to in the original paper were minor stiffening of some vertical tail skin panels which had small cracks. The precise cause was not known. They had no data sheets on the adequacy of design against acoustic fatigue damage.

Concerning measured load information, a limited number of pressure orifices were installed for that purpose. He could vouch for the amount of such data taken to this date. However, structural temperatures were measured on nearly all flights. In addition, strain measurements at low temperatures could also be measured.

He would like to recall one rather interesting event that took place on a flight perhaps a year or so ago. The nose

wheel door was found to gap open slightly and this created a hot spot. To their dismay when they looked into the wheel well after the aircraft had landed, they found molten aluminium alloy splashed around the inside. Luckily the part that melted was some instrumentation tubing—there was no melted structure. This incident really served to illustrate the effects of aerodynamic heating.

A Speaker: He would like to thank Dr. Schleicher for one of the most interesting hours that he had spent for a long time and would like to ask: to what extent was the flight profile controlled by manual means or by automatic means and the value of g achieved in the pull-out?

Dr. Schleicher: The aircraft was completely under the control of the pilot. He had two sets of controls. One was for use when dynamic pressures were high, say below 80 000 feet, where he got good control surface reaction. However, as he got above 100 000 feet, the dynamic pressure dropped off and, as a result, the aircraft depended on jet controls. Jets were located in the nose for pitch and yaw control and another set was located near the wing tips for roll control. The pilot used the ballistic control any time he went over 100 000 feet. He had a normal stick control as well as a wrist control located on a side console, which some of the pilots preferred. Each flight was carefully planned in advance. Even though he had shown them the design altitude mission and a design speed mission, there were several others which they included in the design of the aircraft. Since NASA had been flying the aircraft, North American assisted by investigating and reviewing each of the missions planned, using the data which NASA made available to them. In this way they could advise whether or not the aircraft was capable of going the next mission—This was Research. The acceleration during pull-out was usually less than four g's.

A Speaker: Dr. Schleicher gave a figure for the overall structure weight; could he give them the proportion of the wing and fuselage? In the design of the structure, how much of the structure was designed by strength and how much on stiffness? Did they achieve a balance in this or was there a surplus of strength or a surplus of stiffness? In some of the tests Dr. Schleicher indicated there was no surplus of strength and in other cases there was quite a surplus of strength.

Dr. Schleicher: The structural weight of the wing was 1406 lb, the empennage 1078, fuselage 3812, the landing gear 447 and the surface controls 937 lb. These were the specification weights but the actual weights differed only slightly over those, making the total for the whole aeroplane about 400 lb over the weight shown.

The forward and mid-fuselage structure was designed primarily by the high nose wheel loads during landing at normal temperatures. This gave adequate strength for the hot flight conditions when thermal stresses became additive. The wing was designed for strength plus thermal stresses and, consequently, the resulting torsional stiffness was adequate to meet the flutter requirements. The main emphasis was on flutter stiffness in the design of the horizontal tail. This was the hardest to achieve. The high design pressures in the fuel and oxidiser tanks required sufficient strength to meet the flight load requirements. The larger portion of the total air load that was carried by the fuselage offset the inertia loads along its length. This fact resulted in relatively low bending moments under flight conditions.

A Speaker: Was mass balance used in the prevention of flutter or were all parts of the aeroplane that might be prone to flutter made sufficiently stiff to overcome this phenomena?

Dr. Schleicher: No mass balances were used. All control surfaces had irreversible systems. The hydraulic actuator for the wing flaps had to be increased in size to get adequate stiffness and a lock was installed to hold the flaps rigidly in an up position. For the horizontal tail, one of the design changes they had to make was to move the centre of rotation

from the 35 per cent to the 25 per cent chordline. several iterations of torsional stiffness, the thickness of skins required to hold the maximum temperature to 1200° resulted in adequate strength. All of these parameters were influential in the horizontal tail design problem. The hydraulic cylinder for the horizontal tail was increased purposely in order to get a higher spring rate, but there were no mass balances used.

A Speaker: Could Dr. Schleicher tell them how the temperatures that were presumably calculated in their designs had worked out in relation to what had been measured and therefore, how confident they were in joint conductances?

Dr. Schleicher: Most of the data that he had seen had indicated that the actual measured temperatures fell slightly below the calculated values. However, he could not guarantee that this was completely true in all flight régimes and all parts of the aircraft. So far there had been no serious over-temperature indication that could cause them to be alarmed. They were to please consider this as inconclusive since he could not give a precise answer concerning flight test results. If they wished to learn of the findings resulting from the flight test programme, he would have to refer them to NASA.

A Speaker: How were the transparencies faired and sealed into the frame, bearing in mind the different coefficients of expansion between the transparencies and the frame?

Dr. Schleicher: The transparent material was mechanically retained in the windshield frame with an asbestos fabric cushion.

A Speaker: With reference to the undercarriage test, what method was used to measure the drop velocity?

Dr. Schleicher: The drop velocity was simply a function of the free fall height of the test mass. The nose wheel travel, strut stroke and ground reaction were measured electronically and recorded on an oscillograph. Ground reactions were measured via a calibrated platform.

A Speaker: It appeared that some of the landing problems arose from the fact that the main gear was so far aft of the c.g. and that the second impact load was the design load; could Dr. Schleicher say why the main gear was so far aft of the centre of gravity? His other point, was account taken of the stabilisation of the cover skins by lateral bending stiffness of the corrugated webs and how effective was this in increasing instability strength of a compressive cover?

Dr. Schleicher: They built a scale model of the aircraft representing it dynamically and tested various locations of the main gear and the swivelling nose wheel. This was fired off on a ground catapult along a concrete runway and its course of travel photographed and they found that this particular configuration gave the desired stability. During the tests they reached a scale runout value equivalent of 6000 ft full scale. That was approximately the distance the aircraft utilised on each landing. It varied from 5000 to 7000 ft runout distance. The model remained stable and they had had no problem in landing stability on the aircraft so far.

The corrugated webs were attached to the skin by means of two separate angles which were stiff in themselves and this gave good support. They considered that they had simple support from the closely spaced spars and this nullified any question of actual restraint.

Dr. Schleicher: In reply to a question about honeycomb, there had not been too much work done on honeycomb construction to that point and since they were looking for a material which had high strength characteristics at 1200°F, Inconel X filled that bill very well. They chose to use the multi-spar construction in the wing and Fig. 18 showed the efficiencies they attained with this type of construction. Truthfully, after the skin thicknesses were selected for both strength and torsional rigidity, there was no real need to increase the stiffness any further.

A Speaker: Had fatigue had any significance on the X-15? If so, did they have any data on the fatigue strength of materials at the very high temperatures encountered?

Dr. Schleicher: There was not too much information available on the fatigue characteristics of those materials up to those temperatures. They assumed a comparatively high life for the aircraft and made sufficient investigations to satisfy themselves that they were not in a critical fatigue or creep range. These investigations indicated that at these high temperatures Inconel X gave good fatigue strength. If it were assumed that the aircraft life were 200 hours of flight time, this would be tremendous for this aeroplane, realising that each flight did not last more than ten minutes and about 50 per cent of this was hot. The aeroplane cooled off very rapidly as it got to the landing stage.

A Speaker: In one or two figures there was a difference in temperature between the upper surface and the lower surface, he thought in the order of 250°F; would this difference in temperature cause any distortion due to the eventual expansion of the top surface and bottom surface, and, if so, did this give any adverse aerodynamic effects?

Dr. Schleicher: It gave a slight distortion it was true, but it was extremely minute when one considered that the temperature differential would only be about 200° to 300° over the depth of the wing. They did investigate the deformation in the wing from thermal strains alone and these were not a limiting condition. The wing skins throughout the entire time-temperature-load history remained smooth and there was no buckling of the skin even temporarily. They did, however, in the case of the horizontal tail, permit slight buckling to take place at limit loads but not remain permanent.